麻疹ウイルス F 蛋白の膜融合活性発現の分子機構

Molecular mechanism of expression of membranefusion activity by fusion protein of measles virus

2015 年 3 月

長浜バイオ大学大学院バイオサイエンス研究科

バイオサイエンス専攻バイオ科学技術領域

佐藤 友人

INDEX

INTRODUCTION

Measles virus (MV), a member of the genus *Morbillivirus* in the family *Paramyxoviridae*, is an enveloped virus with a nonsegmented negative-sense RNA genome of about 16,000 nucleotides. The genomic RNA, encapsidated by the nucleocapsid (N) protein, and associated with a virus RNA-dependent RNA polymerase composed of two subunits, the phospho (P)- and large (L) proteins, forms a helical ribonucleoprotein complex (RNP) core of the virus (1). Each virus particle maintains its structure with the matrix (M) protein underlying the lipid bilayer of the envelope on which glycoprotein spikes, the hemagglutinin (H) and fusion (F) proteins, are protruding (2) (Figure A). The initial step of MV infection is attachment to cells via binding of the H protein to cellular receptors (3). Clinical isolates of MV utilize signaling lymphocyte activation molecule (SLAM; also known as CD150) and recently identified nectin4 (PVRL4) as receptors to infect certain types of cells or organs of the immune system (4, 5) and epitherial cells or tissues (6, 7), respectively. Binding of the H protein to a receptor triggers fusion of the virus envelope with the plasma membrane (envelope fusion) (Figure B), a process mediated by the F protein (8), releasing RNP into the cytoplasm. RNP then initiates the transcription of virus mRNAs, and as synthesized virus proteins accumulate, the same RNP comes to be used as the template for synthesis of a positive-strand antigenome, from which virus genome RNA is replicated.

MV spreads in cell cultures or animal tissues in two ways. Besides producing progeny virus particles that undergo multiple cycles of infection via envelope fusion, MV fuses the infected cells directly with neighboring uninfected cell membrane (cell-cell fusion) (Figure C). In either membrane fusion step, the F protein plays a principal role. After synthesized at rough ER as a homotrimer of an inactive precursor, F0, the F protein should be cleaved by furin in the *trans*-Golgi into active complex of disulfide-linked F1 and F2 subunits on the way of the transport to the cell surface (9). The fusion peptides exposed anew at the N-terminus of the F1 subunit is indispensable to exert fusion activity. To promote membrane fusion, the F protein performs conformational change (refolding) from a thermodynamically metastable prefusion form to a highly stable postfusion form, on the way of which it should get over an energetically activated unstable intermediate state (10, 11) (Figure. D, E). The F protein becomes unstable as temperature goes up because its thermodynamic energy level is elevated, therefore, increased temperature lowers this energy barrier and heat treatment at 60℃ induces refolding of the F protein (12). At 37℃, the physiological temperature, however, MV requires an activation signal from the H protein to overcome the energy barrier (12–16).

A series of the refolding process of paramyxovirus F protein has been proposed based on the prefusion and postfusion structures of parainfluenzavirus 5 (PIV5) and human parainfluenzavirus 3 (hPIV3) F proteins, respectively (17, 18). The metastable prefusion form consists of the three-helix bundle, called the stalk region, of the heptad repeat B (HR-B) domain of each subunit of the homotrimer and the head region composed of the DI, DII and DIII domains. Upon activation by the hemagglutinin-neuraminidase protein (an attachment protein corresponding to the H protein of MV), the HR-B domain in the stalk region of the F protein melts and opens breaking its interaction with the head region accompanied by unpacking of the fusion peptide as well as refolding of DIII domain of the head region, resulting in the assembly of the coiled-coil short fragments into a long heptad repeat A (HR-A) domain and translocation of the fusion peptide towards the target cell membrane. The HR-A and HR-B helices of the transiently formed unstable pre-hairpin intermediate are then combined into the stable six-helix bundle to complete the refolding, through which merge of the lipid bilayers could be induced (Figure D). These core processes of the structural change are considered conserved among paramyxoviruses (11, 19–23), and analyses of various MV F protein mutants have specified three major loci implicated in the fusion activity: a cavity in the head region flanked by two different subunits of the F-trimer in which tetrameric H protein-stalks may be lodged (14, 24), and two domains, N-terminal region of the HR-B and microdomain in the DIII adjacent to the HR-A, where the initial conformational changes take place (19, 25–30).

Recently, a variant of a clinical MV lacking cell-cell fusion activity with a single point substitution, N465H, in the HR-B domain of the F protein was isolated. The valiant easily generated revertant viruses that demonstrate cell-cell fusion, and all the five such back mutant viruses carried an additional amino acid substitution in the DIII domain. Whereas Doyle *et al*. reported that amino acid 94 in the DIII domain and 462 in the HR-B domain control the stability and transport competence of the F protein in a correlated manner (28), they did not analyze the precise mechanism. Here, by characterizing the effect of each amino acid substitution on cell-cell fusion activity in relation to thermodynamic stability of the F protein molecule, the molecular mechanism how these amino acid mutations in the HR-B and DIII domains cooperatively modulate fusion activity of the F protein was studied. It was clearly shown that complementation of the stability between the HR-B and DIII domains supports cell-cell fusion activity of the F protein. Based on the analyses of the structural model of the F protein prefusion form, amino acids in the DIII domain that strongly destabilize the F protein revealed to be located in the interface of two subunits being involved in the interaction of each subunit, and amino acid 465 in the HR-B domain was shown to regulate fusion activity depending its molecular volume and the direction

of its side chain.

Figure

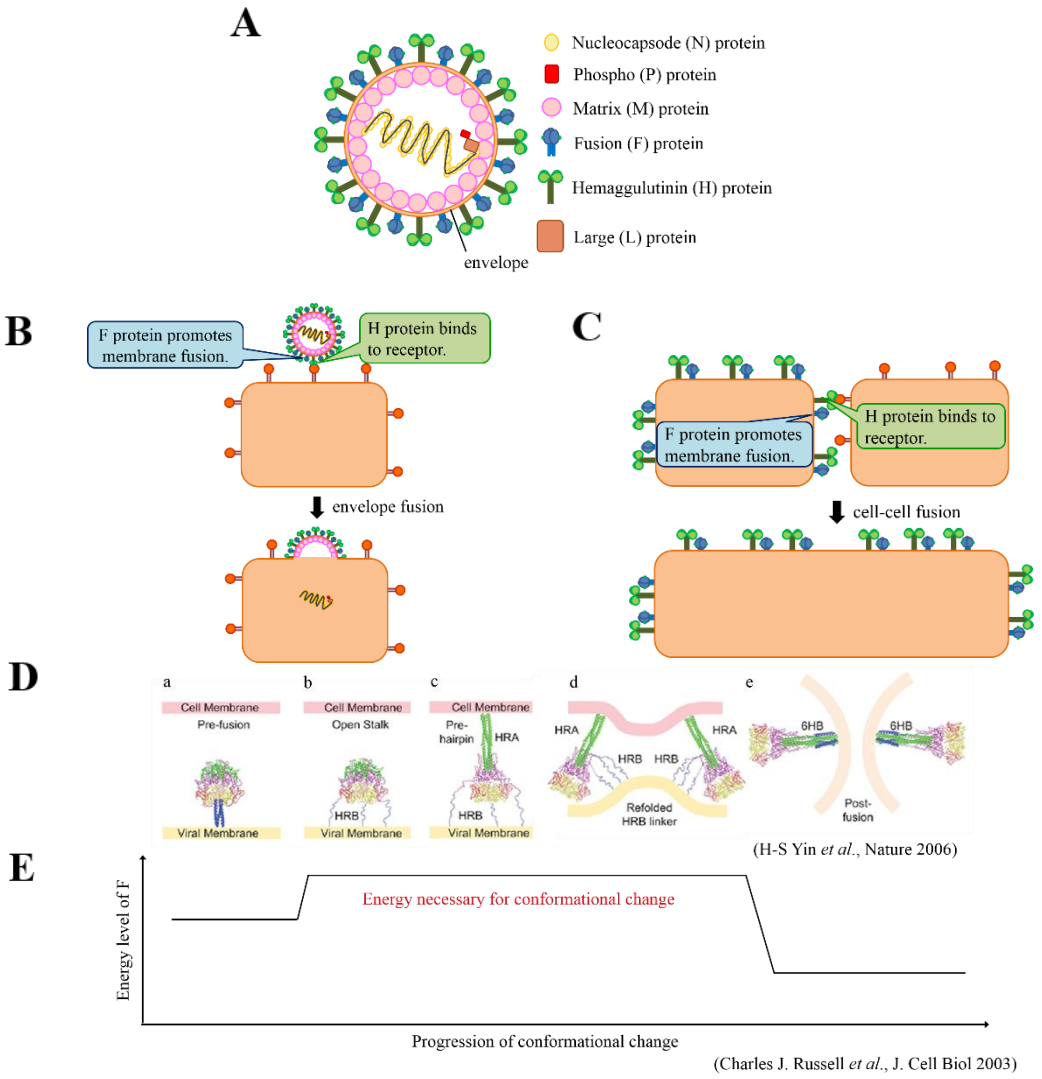

Figure.

Mechanism of membrane fusion induced by measles virus (MV). (A) Structure of MV particle. The hemaggulutinin (H) and the fusion (F) proteins are protruding from viral envelope. (B) Schematic diagram of envelope fusion. The H protein engages in recognition of and binding to a cellular receptor on the target cell surface. The binding is thought to trigger the conformational change of the F protein, which brings viral envelope and plasma membrane of the infected cells together, promoting envelope fusion. (C) Schematic diagram of cell-cell fusion. MV H and F proteins are expressed on the surface of MV-infected cell. The H protein engages in recognition of and binding to a cellular receptor on the neighboring uninfected cell. The binding is thought to trigger the conformational change of the F protein, which brings membranes of the infected and neighboring cells together, promoting membrane fusion. (D) Model of F protein-mediated membrane fusion (17). (a) Structure of the prefusion conformation of the F protein in trimer. (b) 'Open stalk' conformation, in which the helical structure of HR-B stalk melts and the three segments separate from each other. HR-B is shown as three extended chains because the individual segments are unlikely to be helical. (c) A pre-hairpin intermediate formed by refolding of DIII, facilitating formation of the HR-A coiled coil and insertion of the fusion peptides into the target cell membrane. (d) Folding of the HR-B linker, adjacent to HR-B joining it to the head region, onto the newly exposed DIII core with the formation of additional β-strands. (e) Formation of the postfusion 6HB, bundle composed of 3 α-helix strands of each of HR-A and HR-B, juxtaposing the membrane-interacting fusion peptides and transmembrane domains, which is tightly linked to membrane fusion and pore formation. (E) Energy shift of the F protein associated with the conformational change (10). Energy level of the F protein changes with the progression of the conformational change from the metastable prefusion conformation to the stable postfusion conformation beyond the unstable intermediate state. The predicted conformations of the intermediate molecule with high energy are demonstrated in (D) from (b) to (d).

CHAPTER 1

Intramolecular complementation of measles virus fusion protein stability confers the fusion activity at 37℃

1. Abstract

A variant of a clinical MV lacking cell-cell fusion activity with a single point substitution, N465H, in the HR-B domain of the F protein was isolated. The variant easily generated revertant viruses that demonstrate cell-cell fusion, and all the 5 such back mutant viruses carried an additional amino acid substitution, N183D, F217L, P219S, I225T or G240R in the DIII domain of the F protein.

Thermodynamically stabilized by the N465H substitution, the F protein required elevated temperature as high as 40℃ to express cell-cell fusion. The bulky ring of His465 might protect the triple-helix bundle of the HR-B domain from water-mediated dissociation. On the other hand, all the 5 DIII mutations caused destabilization of the F protein allowing the highest fusion activity at 30℃. In a homology-modeled structure of the MV F prefusion form, mutations N183D, P219S and G240R are located in the inter-subunit interface, which could alter the physicochemical properties, such as charge, size and polarity, of the side chains located in the inter-subunit, causing a destabilization of the inter-subunit interaction. Mutations F217L and I225T might make the fusion peptide region more easily dissociate from the head region lowering the energy barrier for refolding of the prefusion form into the postfusion one. The F proteins possessing double mutations both in the HR-B and DIII domains demonstrated efficient cell-cell fusion activities at 37℃. The study here showed that a stabilization effect caused by His465 somehow compensates a destabilization effect caused by each of the DIII mutations to exert cell-cell fusion activity at 37℃ even if the HR-B and DIII domains are distant from each other in the prefusion form.

2. Materials and methods

Cells and viruses. Vero cells constitutively expressing human signaling lymphocyte activation molecule (Vero/hSLAM) (a gift from Y. Yanagi) (31) and Vero cells were maintained in Dulbecco's modified Eagle's medium (DMEM) supplemented with 7% fetal bovine serum (FBS). A marmoset B-cell line cells transformed with Epstein-Barr virus (B95a) were maintained in high-glucose DMEM supplemented with 10% FBS and BHK cells constitutively expressing T7 RNA polymerase (BHK/T7-9) (a gift from N. Ito and M. Sugiyama) (32) were maintained in RPMI 1640 medium supplemented with 8% FBS and 0.6 mg/ml hygromycin B.

The yuKE strain of MV (genotype H1) isolated from a measles patient was passaged once in B95a cells followed by 10 times in Vero/hSLAM cells. The cloned viruses were then obtained by picking either one of the syncytia (clone 1) or blindly the infected cells without syncytium (clone 2). The recombinant MVs (rMVs) were generated according to Seki et al. (33) as described previously (34) using MV full-length genome plasmids. T7 RNA polymerase-expressing vaccinia virus (vTF7-3) (35) was a gift from B. Moss.

Plasmid construction. cDNA of the F protein mRNA of the yuKE strain clone 1 was synthesized by reverse transcription-PCR. The HpaI-PstI fragment (nt 6362 to 7867 according to the IC-B strain genome sequence; GenBank: AB016162) of the p(+)MV323c72-EGFP plasmid (34) derived from the p(+)MV323-EGFP (a gift from Y. Yanagi) (36) was replaced by the corresponding fragment of the clone 1, which generated the full-length genome plasmids p(+)MV323c72-EGFP/F-WT(H1) carrying the wild-type (WT) F gene of the yuKE strain. Amino acid substitutions, N183D, F217L, P219S, I225T, G240R and N465H, were introduced separately or in combination to the p(+)MV323c72-EGFP/F-WT(H1) to obtain the full-length genome plasmids for mutant rMVs.

For expression of proteins using plasmid, cDNA of the WT and mutant F genes as well as the H gene of the yuKE strain were cloned into pcDNA3 plasmid (Invitrogen Life Technologies). In the series of F protein cleavage site mutant, the furin cleavage motif RRHKR (amino acid 108 to 112) was changed to the trypsin cleavage motif VPQSR of Sendai virus (37). To express the bioactive F proteins harboring an engineered FLAG tag in the ectodomain (12), FLAG tag sequence (DYKDDDDK) were inserted in the C-terminal region of the F2 subunit between Val104 and Thr105.

Quantitative cell-cell fusion assay. Vero cells seeded in 24-well plates were

transfected with 0.5 μg each of the F protein- and the H protein-expressing plasmids using polyethyleneimine (Polysciences), infected with vTF7-3 at an multiplicity of infection (MOI) of 2 and incubated at 30 °C or 37 °C. At 24 h post-transfection, the cells were overlaid with Vero/hSLAM cells and further incubated at 30 °C for 18 h, or at 37° C or 40 °C for 12 h in the presence of 100 μM cycloheximide. The cells were fixed, stained with crystal violet and numbers of syncytia and nuclei per syncytium were counted under microscope. Cell-cell fusion activity was shown as the product by multiplying the two values.

Cell surface biotinylation and Western blotting analysis. Vero cells in 24-well plates were transfected with 0.5 μg of the F protein-expressing plasmid using Lipofectamine LTX (invitrogen), infected with vTF7-3 at an MOI of 2 and incubated at 37 °C or 30 °C for 24 h. Then cells were incubated with 0.25 mg of EZ-Link Sulfo-NHS-SS-Biotin (Thermo Scientific) at room temperature for 30 min followed by lysis (150 mM NaCl, 1.0% Triton X-100, 50mM Tris-HCl, pH 8.0) at 4 °C for 1 h. The lysate clarified by centrifugation was mixed with Streptavidin Sepharose High Performance (GE Healthcare Bio-Science) at 4° C for 120 min. The adsorbed biotinylated proteins were subjected to SDS-polyacrylamide gel electrophoresis and electroblotting onto PVDF membranes (GE Healthcare Bio-Science). The F proteins were detected using rabbit polyclonal antibody against MV F protein as the first antibody as described previously (34).

Detection of conformational change of the F protein using a monoclonal antibody by indirect immunofluorescence staining. Vero cells were transfected with 0.5 μg of the F protein-expressing plasmid using Lipofectamine LTX (invitrogen) and incubated at 30℃. At 24 h posttransfection, the transfected cells were transferred to 45℃, 50℃ or 55℃ and kept for 45 min. Subsequently, unfixed and unpermeabilized cells were washed twice with ice-cold PBS and stained with anti-trig F monoclonal antibody (MAb) 16AG5 that binds specifically to an epitope present only in the postfusion (triggered) F structure (a gift from M. Ehnlund) (12, 38) or anti-FLAG MAb M2 (Sigma-Aldrich) followed by incubation with Alexa Fluor 488-conjugated secondary antibody. Images of the positive cells were captured with fluorescence microscope.

Structure modeling of the F protein. Homology-based structure model of prefusion MV F protein was built using the X-ray structure of PIV5 F protein (PDB: 2B9B) (17) with the Molecular Operating Environment software (Chemical Computing Group Inc.). The model structure was evaluated with the 3D profile method (39) implemented in the

Discovery Studio software (Accelrys).

3. Results

Defect of MV cell-cell fusion activity due to the F protein N465H substitution was restored by an additional mutation in the DIII region. From an MV clinical isolate yuKE strain, two clones of viruses were plaque purified: the clone 1 forming large syncytia typical for MV and the clone 2 lacking syncytium formation. The clone 1 possessed Asn465 (GenBank: AB968383) commonly observed in MV WT F proteins, but His465 of the clone 2 was not found in databases. The rMV possessing either the WT or mutant F protein (F-WT or F-N465H) (rMV/F-WT or rMV/F-N465H) certified that the N465H substitution is responsible for the defect of cell–cell fusion activity of the clone 2 (Fig. 1A). The residue 465 is located in the HR-B domain in the stalk region of the MV F protein (Fig. 1D, see Fig. 5A).

The rMV with the mutant F-N465H protein generated revertant viruses that form syncytia. Each of 5 such revertants possessed a single point mutation, N183D, F217L, P219S, I225T or G240R in the DIII domatin in the head region of the F protein (DIII mutations) besides the N465H substitution. rMVs carrying double mutations in the F protein (F-N183D/N465H, F-F217L/N465H, FP219S/N465H, F-I225T/N465H and F-G240R/N465H) confirmed that these DIII mutations were responsible for restoration of cell–cell fusion activity (Fig. 1B). rMVs with a single DIII mutation in the F protein (F-N183D, F-P219S and F-G240R), however, could not be recovered at all, and with F-F217L protein demonstrated small syncytium (Fig. 1C), which suggested that the DIII mutations do not simply enhance the cell–cell fusion activity of the F protein.

The DIII mutations interfere with cleavage of the F protein, which is alleviated by the N465H substitution. Then, the F-N465H protein and the F proteins carrying DIII mutations (DIII mutated F proteins) were expressed using plasmids to characterize their cell–cell fusion activity. The F-N465H protein did not show cell–cell fusion activity (Fig. 2A) although amount of cell surface F1 subunit was comparable with that of the F-WT protein (Fig. 2B). On the contrary, the F-N183D, F-P219S and F-G240R proteins that hindered recovery of rMVs also demonstrated no cell–cell fusion, which might be explained by the drastically decreased F1 subunit expression (Fig. 2A). Fig. 2B indicates that the DIII mutations interfere with the cleavage of the F protein by furin into the fusion-active F1 subunit. Amounts of the F1 subunits as well as the total F proteins (combined F0 and F1 proteins) relative to those of the F-WT protein on the cell surface (Fig. 2B) were equivalent to those in the whole cell lysate (data not shown). The transport efficiency, therefore, of the F proteins including the cleaved forms must not be affected by the

mutations. It should be noted that the trace amounts of the F1 subunit support the relatively high cell–cell fusion activity of the F-F217L and F-I225T proteins, which might be explained by the enhanced specific fusion activities (activity per the amount of F1 subunit) of these F proteins at 37 ℃ (see Fig. 4E). The N465H substitution could alleviate the restricted cleavage of the DIII mutated F proteins, and restored cell–cell fusion activity of the F-N183D/N465H, F-P219S/N465H and F-G240R/N465H proteins. The observation coincides with the cell–cell fusion activities of the rMVs in Fig. 1.

The N183D, P219S and G240R mutations prevent the F protein from holding the proper conformation at 37℃, which is relieved by the N465H substitution. Since the DIII mutations were considered to affect the F protein conformation resulting in furin resistance, the F proteins were expressed at 30℃ to see if they hold proper conformation at lower temperature. As shown in Fig. 3C, the DIII mutated F proteins were more readily cleaved by furin at 30℃, and accordingly, the F-N183D, F-P219S and F-G240R proteins restored cell–cell fusion activity (Fig. 3A). These 3 F proteins, however, did not show cell–cell fusion activity at 37℃ (Fig. 3B), which indicates that the 3 F proteins once synthesized correctly at 30℃ should be unstable and easily lose the proper conformation to exert cell–cell fusion at 37℃. On the other hand, the F-F217L and F-I225T proteins expressed at 30℃ demonstrated cell–cell fusion activity at 37℃ suggesting that they maintain correct conformation at 37℃. Although all the 5 DIII mutations alter the F protein conformation inducing furin resistance, each F protein molecule varies in stability at 37℃. In contrast, the F-N465H protein demonstrated no cell–cell fusion activity at 30℃ regardless of its proper conformation to be cleaved. Defect of the F-N465H protein in cell–cell fusion activity at 37℃ might not be caused by instability of the protein. The eliminated cell–cell fusion activity of the F-N183D, F-P219S and F-G240R proteins at 37 ℃ was restored when N465H substitution was additionally introduced (F-N183D/N465H, F-P219S/N465H and F-G240R/N465H proteins), which suggests that N465H substitution should play a role to support the F protein structure in proper conformation.

Cell-cell fusion activity of the F-N465H protein and the DIII mutated F proteins are reciprocally temperature dependent. To compare accurate temperature dependence of the cell–cell fusion activity between the F-N465H and the DIII mutated F proteins, the cleavage site of each F protein was changed to that of Sendai virus so as to be cleaved by supplemented trypsin but not spontaneously by cellular furin (37). When the F proteins with the cleavage site mutation are expressed at 30℃ and cleaved by trypsin before

temperature shift, the system could exclude the influence of the F proteins synthesized de novo because such F proteins would not be cleaved into the fusion-active form.

As shown in Fig. 4A–C, cell–cell fusion activity of the F-WT protein was enhanced as the temperature increased, and the F-N465H protein exhibited the activity only when temperature was as high as 40℃. These two F proteins required higher temperature to perform refolding more efficiently. Contrarily, cell–cell fusion activities of all the DIII mutated F proteins decreased as the temperature increased. The F-N183D, F-P219S and F-G240R proteins lost the activity at 37℃, and the F-F217L and F-I225T proteins showed some restricted activity at 37℃ but not at 40℃. The results demonstrate that the proper conformation of these DIII mutated F proteins once constructed at 30℃ was lost at higher temperatures. On the other hand, significantly high specific fusion activities (activity per the amount of F1 subunit in Fig. 4D) of all the DIII mutated F proteins at 30℃ and of the F-F217L and F-I225T proteins at 37℃ suggest that the DIII mutated F proteins more readily induce membrane fusion than the F-WT protein at low temperatures (Fig. 4E). The F proteins carrying one of the DIII mutations and N465H substitution demonstrated cell–cell fusion activity at any temperature with the highest value at 37℃.

Thermodynamic stability of the mutated F proteins evaluated by the protein conformation using monoclonal antibody. In the recent report, Ader *et al*. (12) successfully identified the conformation of MV F protein using monoclonal antibodies (MAbs) that allow the differentiation of prefusion and postfusion forms and evaluated thermodynamic stability of the F protein. Whereas anti-MV F MAb 186CA recognizes only prefusion conformation of the F protein, MAb 16AG5 binds specifically to an epitope present only in the postfusion (triggered) F structure. Since MAbs specific for the prefusion structure are no more available, the triggered form of the F proteins was detected to study their thermodynamic stability. For detection of the F protein equally under all conditions, the bioactive F proteins harboring an engineered FLAG tag in the ectodomain (12), the linear epitope of which is recognized by an anti-FLAG MAb M2, was employed. To trigger F refolding and drive the prefusion conformation into that of postfusion, the transfected cells were subjected to a brief (45 min) heat shock of 45℃, 50℃ or 55℃. Then the reactivity against the anti-triggered F MAb 16AG5 or anti-FLAG tag MAb M2 was observed by immunofluorescence analysis.

The anti-triggered F MAb 16AG5 detected neither of the F-WT nor the F-N465H proteins after exposure to 45℃ as well as in the absence of the heat shock (Fig. 5). When the cells expressing either of these F proteins were treated at 50℃ or 55℃, the cells obtained the reactivity to the MAb 16AG5, which shows that the conformation of the F

proteins was converted to that of the triggered F protein, although the conversion of the F-N465H protein at 50℃ was restricted compared with that of the F-WT protein. It indicates that N465H mutation raises energy barrier for conformational change of the F protein. On the other hand, the F-G240R protein, a DIII mutant, was detected even in the absence of the heat shock. When the N465H substitution was additively introduced, the F-G240R+N465H protein demonstrated lower reactivity to the MAb 16AG5 than the F-G240R protein after treatment at 45℃ and 50℃. These results ensure that the lowered energy barrier by the G240R mutation was raised by the N465H substitution, suggesting that these amino acid mutations in the DIII and HR-B domains cooperatively modulate energy barrier for conformational change of the F protein.

Residues 183, 219 and 240 are located on the interface of the F protein monomers. On the model structure of the MV F prefusion form constructed using the crystal structure of the PIV5 F protein, residues 183, 219 and 240 are located in the inter-subunit interface of the F protein trimer and in close proximity of amino acids of the neighboring subunit chains (Fig. 6B). These amino acids should be involved in the mutual interaction of the subunits. On the other hand, residues 217 and 225 are almost buried in a subunit and are surrounded by hydrophobic residues (Fig. 6C).

4. Discussion

The membrane fusion process of paramyxovirus is driven by a drastic conformational change of the F protein from a metastable prefusion to a highly stable postfusion form, on the way of which the molecule should get over a thermodynamically activated unstable intermediate state (10, 11, 40, 41). To overcome this energy barrier, MV F protein requires an activation signal from the H protein at 37℃ (12–16). Heat treatment at 60℃, however, has been shown to serve as a surrogate for the H-mediated F activation (12), which implys that the raised temperature decreases the conformational stability of the F prefusion form lowering the energy barrier to the postfusion form. The same effect would explain the enhanced cell–cell fusion activity of the F-WT protein at higher temperatures shown in Fig. 4A–C.

Most of the mutations in the HR-B domain reported up to now stimulate cell–cell fusion activity (29, 30, 42). N462K, one of suchsubstitutions, is thought to destabilize the hydrophobic interaction associating the HR-B/HR-B-linker domains with the head region in the F prefusion form (19). Contrarily, N465H should somehow increase the conformational stability of the F prefusion form, since it inhibited the fusion activity at 37℃ but 40℃ (Fig. 4A–C). The bulky ring of H465 might protect the triple-helix bundle of the HR-B domain from water-mediated dissociation.

On the other hand, cell–cell fusion activity of the DIII mutated F proteins decreased as temperature increased (Fig. 4A–C). Reactivity to the monoclonal antibody recognizing the F postfusion form (12, 21) suggested spontaneous refolding of the F-G240R protein to the postfusion form at 45℃ (Fig. 5), an useless event for the membrane fusion. At lower temperatures, however, they exhibited extremely high specific fusion activities (Fig. 4E). Therefore, each DIII mutation would be considered as a destabilization factor lowering the energy barrier to the postfusion form, which enhances the fusion process unless too high temperature further lowers the energy barrier too much, inducing the wasteful spontaneous refolding.

Destabilization mechanisms of the DIII mutations might not be equal. One group of the mutations (N183D, G240R, P219S) has a destabilization effect to lose the fusion activity due to the spontaneous refolding at lower temperature than the other group (F217L and I225T) (Fig. 6A–C). In a homology-modeled structure of the MV F prefusion form, the former mutations are located in the inter-subunit interface, whereas, the positions of the latter are buried in a subunit and close to the fusion peptide region (Fig. 6B and C). Mutations N183D, G240R and P219S alter the physicochemical properties, such as charge, size and polarity, of the side chains located in the inter-subunit, which

could be a cause to destabilize the inter-subunit interaction (Fig. 6B). On the other hand, mutation I225T breaks the hydrophobic interaction between I225 and a part of the fusion peptide region (L123 and L137), and mutation F217L possibly affects the positioning of the beta-sheet which is in contact with both F217 on one side and another part of the fusion peptide region (S144 and I147) on the other side, weakening the interaction between the beta-sheet and fusion peptide (Fig. 6C). Thus, these mutations could make the fusion peptide region more easily dissociate from the head region.

Doyle *et al.* has demonstrated (28) that residues 462 in the HR-B and 94 in the DIII domains are involved jointly in conformational destabilization that links suppressed cell–cell fusion activity. In the present study, by the addition of the N465H substitution in the HR-B, the DIII mutated F proteins restored cell–cell fusion activity at 37℃, which indicates that, even if the HR-B and DIII domains are distant from each other in the prefusion form, a stabilization effect caused by H465 somehow compensates a destabilization effect caused by each of the DIII mutations to exert cell–cell fusion activity at 37℃.

5. Figures

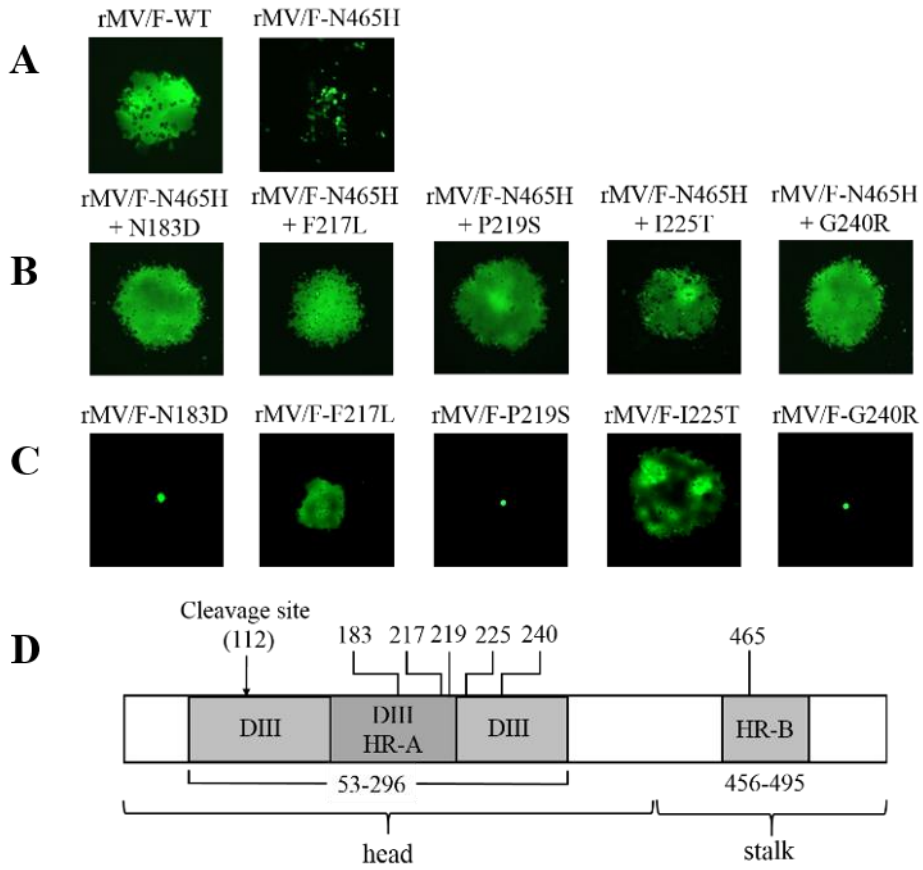

Figure 1.
Abrogation of MV cell-cell fusion by N465H substitution in the F protein. (A) Cytopathic effect of the cells infected with rMV/F-WT or rMV/F-N465H. B95a cells were infected with EGFP-expressing rMV carrying the F-WT protein or F-N465H protein and fixed with 1% paraformaldehyde at 72 h p.i. EGFP expression in the infected cells was observed under a fluorescence microscope. Magnification; x200. (B) Infectious virus titer of the rMV/F-WT and rMV/F-N465H. Vero/hSLAM cells were infected with rMV/F-WT or rMV/F-N465H at an MOI of 0.01. At 72 h p.i., the infectious viruses in the culture medium were titrated. (C) Localization of residue 465 in the pre-fusion form of MV F protein structure. A schematic diagram of the domains of MV F protein (upper), surface model of the constructed pre-fusion form of MV F protein-trimer (lower left), and close-up view of N-terminal region of the HR-B domain in ribbon model (lower right) are shown. Residues 465 (marked in red) and 462 (marked in green) are located side by side in the HR-B stalk domain.

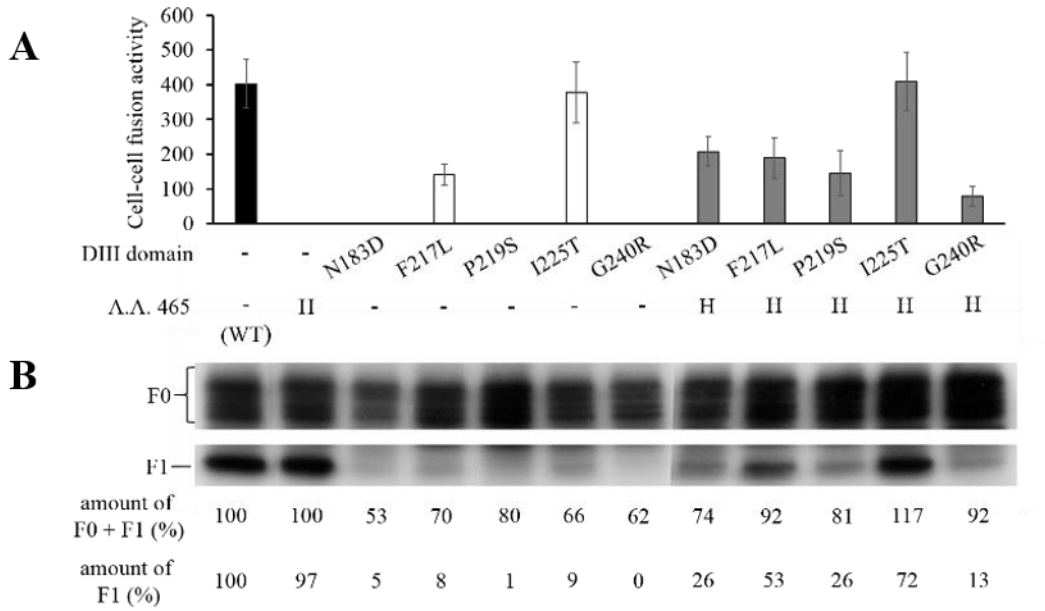

Figure 2.

Effect of the N465H substitution and the DIII mutations on fusion function of the F protein. (A) Cell-cell fusion activities of the F proteins. Vero cells were transfected with a plasmid expressing one of the F proteins together with the H protein-expressing plasmid and incubated at 37℃ for 24 h. Then the cells were overlaid with Vero/SLAM cells, incubated further 12 h and stained with crystal violet. Numbers of syncytia and nuclei in each syncytium were counted under microscope, and cell-cell fusion activity is demonstrated by multiplying these two parameters. Black column, F-WT or F-N465H protein; white column, DIII mutated F proteins; gray column, doubly mutated F proteins with N465H substitution and one of the DIII mutations. (B) Cell surface expression of the F proteins at 37℃. Vero cells were transfected with the F protein-expressing plasmids, incubated at 37℃ for 24 h, and then biotinylated and lysed. Biotinylated cell surface proteins were precipitated with streptavidin-coated sepharose beads, and subjected to immunoblot analysis using rabbit polyclonal antibody against the F protein. Combined amount of F0 and cleaved F1 proteins was shown as the total F protein. Amounts of the mutant F proteins were demonstrated relative to that of the F-WT protein.

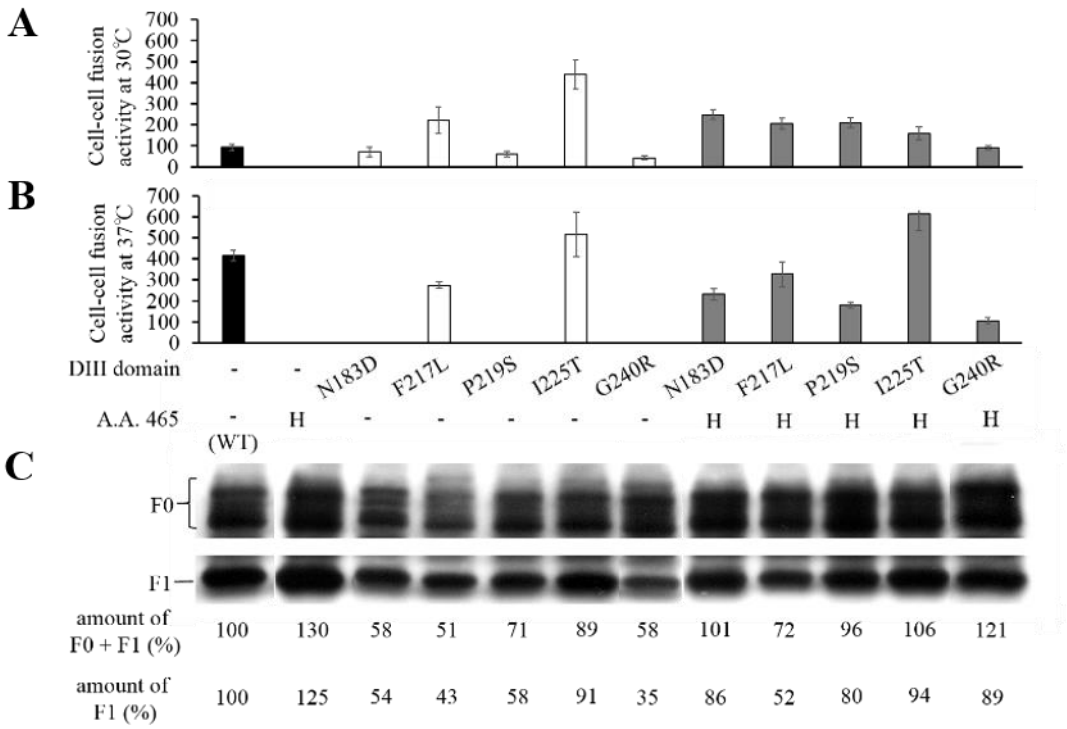

Figure 3.

Effect of the lowed temperature on fusion function of the F proteins. (A and B) Cell-cell fusion activities of the F proteins synthesized at 30℃. Vero cells were transfected with a plasmid expressing one of the F proteins together with the H protein-expressing plasmid and incubated at 30℃ for 24 h. Then the transfected Vero cells were overlaid with Vero/SLAM cells and incubated continuously at 30℃ further 18 h (A) or at 37℃ for 12 h (B) in the presence of 100 μM cycloheximide. Cells were fixed and stained and cell-cell fusion was quantified as described in Fig. 2 (A). (C) Cell surface expression of the F proteins at 30℃. Vero cells were transfected with the F protein-expressing plasmids, incubated at 30℃, biotinylated at 24 h posttransfection, and lysed. Biotinylated cell surface proteins were analyzed by immunoblotting as described in Fig. 2(B).

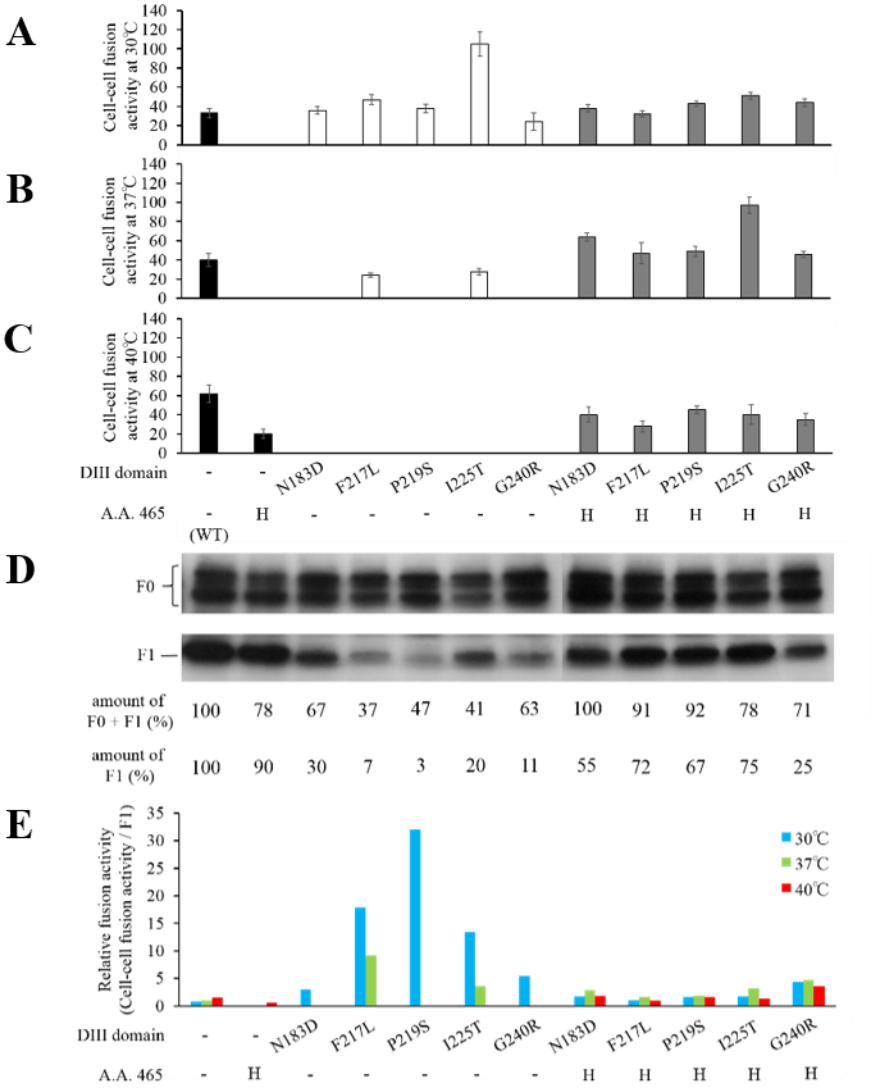

Figure 4.

Temperature dependence of fusion function of the F proteins. (A-C) Cell-cell fusion activities of the F proteins evaluated using cleavage site mutated F proteins. Vero cells were transfected with a plasmid expressing one of the F proteins together with the H protein-expressing plasmid and incubated at 30℃. At 24 h posttransfection, the culture medium was replaced with the medium including 1 μg/ml trypsin and incubated 37 ℃ for 1 h. Then the cells were overlaid with Vero/SLAM cells and continuously incubated at 30℃ for 18 h (A), or transferred to 37℃ (B) or 40℃ (C) and incubated for 12 h in the presence of 100 μM cycloheximide and trypsin inhibitor. At 18 h or 12 h post cocultivation, cell-cell fusion was evaluated as described in Fig. 2(A). (D) Cell surface expression of the cleavage site mutated F proteins at 30℃. Vero cells were transfected with a plasmid expressing cleavage site mutated F protein and incubated at 30℃. At 24 h posttransfection, the culture medium was replaced with the medium including 1μg/ml trypsin and incubated 37 ℃ for 1 h. Then the cell surface proteins were biotinylated and analyzed by immunoblotting as described in Fig. 2(B). (E) Specific cell-cell fusion activity of the F proteins. Specific cell-cell fusion activities were calculated by dividing cell-cell fusion activity at each temperature (A-C) by the amount of cleaved F1 subunit (D).

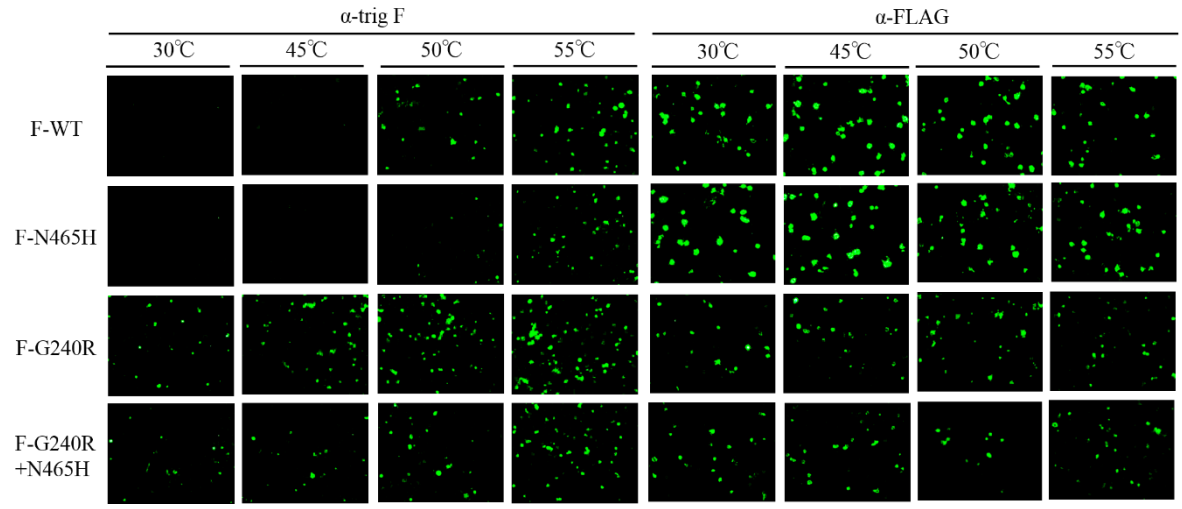

Figure 5.
Evaluation of thermodynamic stability of the mutated F proteins using anti-trig F MAb. Vero cells were transfected with a plasmid expressing one of the mutated F proteins and incubated at 30℃. At 24 h posttransfection, transfected cells were heat treated at 45℃, 50℃ or 55℃ for 45 min. Subsequently, unfixed and unpermeabilized cells were stained with anti-trig F or anti-FLAG MAb for 1 h at 4℃ followed by incubation with Alexa Fluor 488-conjugated secondary antibody. Images of the positive cells were captured with fluorescence microscope.

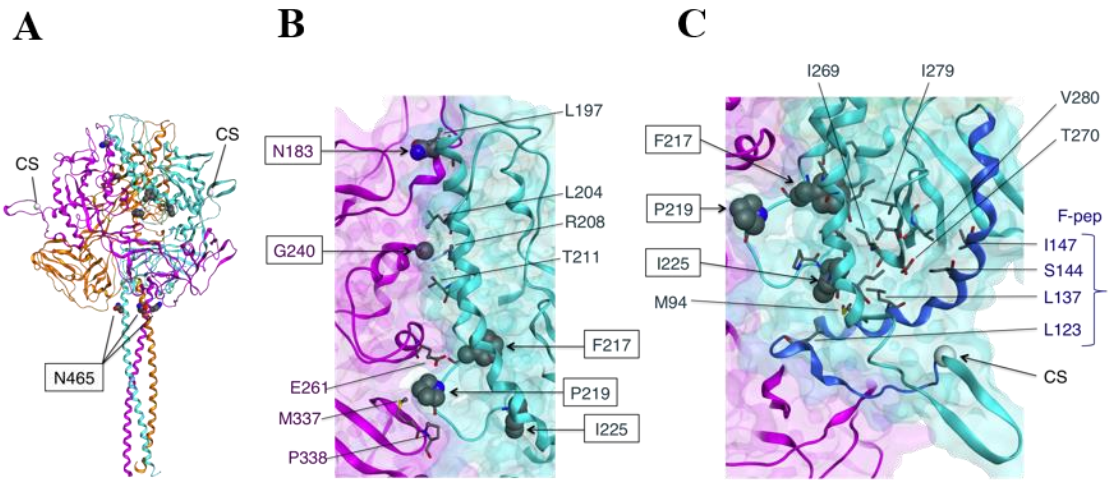

Figure 6.
Mutation sites mapped in a model structure of the MVF pre-fusion form. (A) Overall view. Shown are the main chains in ribbon representation colored by subunit, mutation sites in sphere representation colored by atom, and the cleavage sites (CS) as white spheres. N465 is located in the interface between the head and stalk regions. The other mutation sites studied are in the head region. (B) Close-up view of the mutation sites in the head region. In addition to the same representation elements as in A, Connolly surface of each subunit is semi-transparently shown. N183, G240 and P219 are located in the inter-subunit interface, whereas F217 and I225 are almost completely buried in a subunit. Residues in inter-subunit contact with N183, G240 and P219 are shown in stick representation colored by atom. They are L197 for N183; L204, R208 and T211 for G240; and E201, M337 and P338 for P219. (C) Close-up view of F217 and I225. Basically, the same representation is employed as in B. The F-peptide region (F-pep) is shown in ribbon representation of a dark shade of blue. The stick representation is used for showing hydrophobic residues surrounding F217 and I225 (namely, V83, L84, I87, A90, L91, M94, L123, L137, I213, L216, P224, I269, V272 and I279), and also showing related residues (T270, V280, S144 and I147). Among the residues in F-pep (L123, L137, S144 and I147), L123 and L137 are in contact with I225; S144 and I147 are in contact with residues (T270 and V280, respectively) in such a beta-sheet that also contain residues (I269 and I279) in contact with F217.

CHAPTER 2

Molecular volume and direction of the side chain of amino acid 465 of measles virus fusion protein regulate fusion activity

1. Abstract

An MV variant that lacks cell-cell fusion activity possessed a single point mutation N465H in the HR-B domain of the F protein. Although the HR-B domain is known to be involved in the regulation of fusion activity, all the mutations identified up to now in this domain facilitated fusion activity and N465H is the first mutation that reduces fusion activity.

To examine the characteristics of amino acid 465 related to the control of the fusion activity, Asn465 of the F protein was substituted by various amino acids. The fusion activity of each F protein showed good correlation with the side chain length from the Cα of each residue ($p<0.01$) and van der Waals volume, an indicator of physical mass calculated based on van der Waals radius of atoms consisting the molecule ($p<0.001$), except for Phe, Tyr, Trp, Pro and His carrying ring structures. The F proteins possessing larger mass of amino acids at residue 465 induced cell-cell fusion more readily at 30℃ than at 37℃, which suggests that large molecular volume of amino acid 465 lowers the energy barrier for refolding of the F protein to induce cell-cell fusion. On the other hand, the F proteins with the 5 ring-type amino acids required higher temperature, much more energy, to exert cell-cell fusion.

From the analyses of the structural effects of substitutions at position 465 using the structure model of MV F protein, longer side chains of the non-ring-type amino acids were found to protrude more deeply into the head region and may disturb the hydrophobic interaction between the stalk and head regions and cause destabilization of the molecule conferring the F protein the enhanced cell-cell fusion activity. In the case of ring-type residues, excluding Pro, their side chain turned away from the head region of the prefusion form, resulting in not only no contact with the head region but also extensive coverage of the HR-B surface, which may stabilize the helix bundle and prevent the dissociation of the HR-B bundle, for the membrane fusion process. These results demonstrate that amino acid 465 in the HR-B domain of MV F protein plays a definitive role in regulating fusion activity.

2. Materials and methods

Cells and viruses. Vero cells constitutively expressing human signaling lymphocyte activation molecule (Vero/hSLAM) (a gift from Y. Yanagi) (31) and Vero cells were maintained in Dulbecco's modified Eagle's medium (DMEM) supplemented with 7% fetal bovine serum (FBS). A marmoset B-cell line cells transformed with Epstein-Barr virus (B95a) were maintained in high-glucose DMEM supplemented with 10% FBS and BHK cells constitutively expressing T7 RNA polymerase (BHK/T7-9) (a gift from N. Ito and M. Sugiyama) (32) were maintained in RPMI 1640 medium supplemented with 8% FBS and 0.6 mg/ml hygromycin B.

The yuKE strain of MV (genotype H1) isolated from a measles patient was passaged once in B95a cells followed by 10 times in Vero/hSLAM cells. The cloned viruses were then obtained by picking either one of the syncytia (clone 1) or blindly the infected cells without syncytium (clone 2). The recombinant MVs (rMVs), rMV/F-WT and rMV/F-N465H possessing the wild-type F (WT-F) and the N465H-mutated F (F-N465H) proteins, respectively, were generated according to Seki et al. (33) using MV full-length genome plasmids described below (34). T7 RNA polymerase-expressing vaccinia virus (vTF7-3) (35) was a gift from B. Moss.

Plasmid construction. cDNA of the F protein mRNA of the yuKE strain clone 1 was synthesized by reverse transcription-PCR. The HpaI-PstI fragment (nt 6362 to 7867 according to the IC-B strain genome sequence; GenBank: AB016162) of the p(+)MV323c72-EGFP plasmid (34) derived from the p(+)MV323-EGFP (a gift from Y. Yanagi) (36) was replaced by the corresponding fragment of the clone 1, which generated the full-length genome plasmids p(+)MV323c72-EGFP/F-WT(H1) carrying the WT-F gene of the yuKE strain. Amino acid substitutions, N465H was introduced to the p(+)MV323c72-EGFP/F-WT(H1) to obtain the full-length genome plasmid p(+)MV323c72-EGFP/F-N465H for the clone 2.

For expression of proteins using plasmid, cDNA of the WT and mutant F genes as well as the H gene of the yuKE strain were cloned into pcDNA3 plasmid (Invitrogen Life Technologies, xxxx). To express the bioactive F proteins harboring an engineered FLAG tag in the ectodomain (12), FLAG tag sequence (DYKDDDDK) were inserted in the C-terminal region of the F2 subunit between Val104 and Thr105.

Virus titration. Monolayers of Vero/hSLAM cells in 24-well plates were infected with serially diluted virus samples. After 1 h of incubation at 37℃, the virus samples were

removed, and the cells were overlaid with DMEM containing 7% FBS and 2.5% methylcellulose. At 3 days postinfection (72 h p.i.), virus titer was determined by counting the number of EGFP expressing plaques under a fluorescence microscope (Axioskop; Zeiss, Goettingen, Germany).

Quantitative cell-cell fusion assay. Vero cells seeded in 24-well plates were transfected with 0.5 μg each of the F protein- and the H protein-expressing plasmids using polyethyleneimine (Polysciences, Warrington, PA), infected with vTF7-3 at an multiplicity of infection (MOI) of 2 and incubated at 37℃. At 24 h post-transfection, the cells were overlaid with Vero/hSLAM cells and further incubated at 30℃ for 18 h, or at 37℃ or 40℃ for 12 h in the presence of 100 μM cycloheximide. The cells were fixed, stained with crystal violet and numbers of syncytia and nuclei per syncytium were counted under microscope. Cell-cell fusion activity was shown as the product by multiplying the two values.

Evaluation of the F protein stability. Thermodynamic stability of the F protein mutants was evaluated based on temperature-dependence of the cell-cell fusion activity relative to that of the wild-type F (F-WT) protein according to the method reported previously (19, 43). Relative cell-cell fusion activity was calculated by dividing the cell-cell fusion activity of each F protein mutant at 30℃, 37℃ and 40℃ by that of the F-WT protein at the same temperature, respectively. Stability of the mutant F protein was assessed as follows: destabilized when the relative cell-cell fusion activity was higher at 30℃ than at 37℃, and stabilized when the relative activity at 40℃ was higher than that at 37℃.

Cell surface biotinylation and Western blotting analysis. Vero cells in 24-well plates were transfected with 0.5 μg of the F protein-expressing plasmid using Lipofectamine LTX (Invitrogen), infected with vTF7-3 at an MOI of 2 and incubated at 37℃ for 24 h. Then cells were incubated with 0.25 mg of EZ-Link Sulfo-NHS-SS-Biotin (Thermo Scientific) at room temperature for 30 min followed by lysis (150 mM NaCl, 1.0% Triton X-100, 50mM Tris-HCl, pH 8.0) at 4℃ for 1 h. The lysate clarified by centrifugation was mixed with Streptavidin Sepharose High Performance (GE Healthcare Bio-Science) at 4℃ for 120 min. The adsorbed biotinylated proteins were subjected to SDS-polyacrylamide gel electrophoresis and electroblotting onto PVDF membranes (GE Healthcare Bio-Science). The F proteins were detected using rabbit polyclonal antibody against MV F protein as the first antibody as described previously (34).

Detection of conformational change of the F protein using a monoclonal antibody by indirect immunofluorescence staining. Vero cells were transfected with 0.5 μg of the F protein-expressing plasmid using Lipofectamine LTX (Invitrogen) and incubated at 37℃. At 24 h posttransfection, the transfected cells were transferred to 45℃, 50℃ or 55℃ and kept for 45 min. Subsequently, unfixed and unpermeabilized cells were washed twice with ice-cold PBS and stained with anti-trig F monoclonal antibody (MAb) 16AG5 that binds specifically to an epitope present only in the postfusion (triggered) F structure (a gift from M. Ehnlund) (12, 38) or anti-FLAG MAb M2 (Sigma-Aldrich) followed by incubation with Alexa Fluor 488-conjugated secondary antibody. The number of the positive cells was counted under fluorescence microscope.

Structure modeling of the F protein. Homology-based structure model of prefusion MV F protein was built using the X-ray structure of PIV5 F protein (PDB: 2B9B) (17) with the Molecular Operating Environment software (Chemical Computing Group Inc.). The model structure was evaluated with the 3D profile method (39) implemented in the Discovery Studio software (Accelrys).

Correlation of fusion activity data with various amino acid indices. Pearson's correlation coefficients between the fusion activity value of mutant MV F proteins at 37°C and 30°C, and various amino acid indices were calculated. The amino acid indices represent biochemical and physicochemical properties of amino acids, such as secondary structure propensities, hydrophobicity and structural flexibility. Employed was AAindex database (44), which contains 544 amino acid indices. In addition, other amino acid indices related to side chain flexibility (45, 46, 47), backbone flexibility (46) and the 3D-1D scores (48) were also employed.

3. Results

Growth feature of the rMV/F-N465H. Fig. 1A demonstrates cytopathic effect (CPE) of the rMV/F-N465H compared with that of the rMV/F-WT, confirming that defect of cell-cell fusion activity was due to the N465H substitution in the F protein. Progeny virus production of the rMV/F-N465H, however, was comparable with that of the rMV/F-WT (Fig. 1B), suggesting that such MVs possessing the F-N465H protein as clone 2 isolated from clinical virus (see CHAPTER 1) as well as rMV/F-N465H should spread their infection by releasing infectious particles. It is unknown whether clone 2 originally contaminated in the clinical specimen and originated from an MV patient or emerged during the passage in the laboratory. Since the CPE of the MVs with the F-N465H protein is quite mild, it is possible to recognize such variants only when they carry EGFP gene as rMV.

The amino acid 465 of the F protein is located in the HR-B domain at the junction between the stalk and the head regions just one turn away of amino acid 462 from the head region that was reported to be involved in the fusion activity of the F protein (19) (Fig. 1C).

Cell-cell fusion activity of the F protein is closely related with the molecular volume of amino acid 465 in the HR-B domain. To examine the characteristics of amino acid 465 related with fusion activity, Asn465 of the F-WT protein was substituted by various amino acids (465-mutated F proteins). Each mutant F protein was expressed together with the H protein of the yuKE strain using the pcDNA3 expression vector in Vero cells infected with T7 RNA polymerase-expressing vaccinia virus, and fusion activity was evaluated by counting the number of nuclei in syncytia after overlaying Vero/SLAM cells. Substitution of Asn465 by Arg, Lys, Ile, Gln, or Leu increased fusion activity by approximately two-fold, but that by Phe or Tyr resulted in less than half the fusion activity of the F-WT protein. Especially, the F protein with Trp, Pro or His substitution showed trace or no fusion activity (Fig. 2A). The F protein is synthesized as inactive precursor, F0, and activated by furin into disulfide-linked F1 and F2 subunits (49). The cell surface expressions of the active F1 subunit and total F protein (combined amount of F1 and F0 proteins) of each mutant F protein were not significantly different, which could not explain the change of fusion activity (Fig. 2B). Here it was noticed that the F proteins demonstrating strong fusion activity carry amino acid 465 with relatively long side chains. As shown in Fig. 2C, left panel, cell-cell fusion activity and the length of the side chain from Cα measured on the constructed model showed good correlation

(p<0.01), and when fusion activity was plotted against Van der Waals volume, an indicator of physical mass calculated based on Van der Waals radius of atoms, the correlation became stronger (p<0.001) only if 5 amino acids demonstrated the lowest fusion activity were excluded (Fig. 2C, right panel). These 5 amino acids revealed to carry ring structures (ring-type amino acids): imidazoyl group of His, pyrrolidine ring of Pro, indole group of Trp, and phenyl group of Tyr and Phe.

Large molecular volume of non-ring-type amino acid 465 lowers the energy barrier for refolding of the F protein, whereas ring-type amino acids stabilize the F protein. Fusion activity of MV F protein is enhanced by N462S or N462K substitution in the HR-B helix that destabilizes the molecule (10). Since amino acid Asn465 is located just one turn away (about 4 Å) of Asn462 from the head region (Fig. 1B), fusion activity of each 465-mutated F protein was analyzed at 30℃ to examine whether the substitution affects the stability of the F protein (Fig. 2A). It was found that relative cell-cell fusion activities of the 465-mutated F proteins to that of the F-WT protein increased more prominently at 30℃ as the length of the side chain became longer (Fig. 2D). The ratio of the relative fusion activity at 30℃ to that at 37℃ is in good correlation especially with Van der Waals volume (p<0.01), which indicates that the F proteins possessing amino acid 465 of larger volume induce cell-cell fusion more readily at low temperature (Fig. 2E). The result suggests that large molecular volume of amino acid 465 lowers the energy barrier for the conformational change of the F protein to induce cell-cell fusion.

Five 465-mutated F proteins with a ring-type amino acid were excluded from the fusion analyses at 30℃ as their fusion activities were extremely restricted and independent of Van der Waals volume (Fig. 2C). Then, fusion assay of these F proteins was performed at higher temperature. The F-N465W, F-N465P and F-N465H proteins that hardly expressed cell-cell fusion activity at 37℃ formed tiny syncytia at 40℃ (Fig. 2F, upper panel). Relative fusion activities of these mutant F proteins normalized to that of the F-WT protein were reduced, contrarily to the F-N465K protein whose relative activity was stimulated, as temperature decreased (Fig. 2F, lower panel). The result suggests that these 5 ring-type amino acids at position 465 stabilize the F protein and raise energy barrier for conformational change of the F protein.

Thermodynamic stability of the 465-mutated F proteins evaluated by the protein conformation using monoclonal antibody. In the recent report, Ader *et al*. (12) successfully identified the conformation of MV F protein using monoclonal antibodies (MAbs) that allow the discrimination of prefusion and postfusion forms and evaluated

thermodynamic stability of the F protein. Whereas anti-MV F MAb 186CA recognizes only pre-fusion conformation of the F protein, MAb 16AG5 binds specifically to an epitope present only in the postfusion (triggered) F structure. Since MAbs specific for the pre-fusion structure are no more available, the triggered form of the 465-mutated F proteins was detected to study their thermodynamic stability. For detection of the F protein equally under all conditions, the bioactive F proteins harboring an engineered FLAG tag in the ectodomain (12), the linear epitope of which is recognized by an anti-FLAG MAb M2, was employed. To trigger F refolding and drive the prefusion conformation into that of postfusion, the transfected cells were subjected to a brief (45 min) heat shock of 45℃, 50℃ or 55℃. Then the reactivity against the anti-triggered F MAb 16AG5 or anti-FLAG tag MAb M2 was observed by immunofluorescence analysis. The remaining cell-cell fusion activity after the heat shock was also estimated.

The anti-triggered F MAb 16AG5 detected none of the F-N465K, F-N465T, F-WT(Asn465), F-N465G and F-N465F proteins after exposure to 45℃ as well as in the absence of the heat shock (Fig. 3A). When the cells expressing one of these F proteins were treated at 50℃ or 55℃, the F proteins obtained the reactivity to the MAb 16AG5, which shows that their conformation were converted to those of the triggered F protein. The number of the cells detected by anti-triggered F MAb in Fig. 3A was counted under fluorescence microscope and demonstrated in Fig. 3B. It is clearly shown that the F-N465K protein was most easily converted to the triggered conformation and that the number of anti-triggered F MAb positive cells decreased as the molecular volume of the amino acid 465 reduced, to the smallest count of the F-N465F protein, a ring-type amino acid. The result is in good correlation with the cell-cell fusion activity shown in Fig. 2A. As the control, cells were stained with the anti-FLAG MAb recognizing a linear epitope, which returned indistinguishable staining under all conditions. Furthermore, the cell-cell fusion activities of the 465-mutated F proteins remaining after the heat shock were examined (Fig. 3C). Fig. 3D showed relative cell-cell fusion activity of these 5 F proteins normalized to that without heat shock. Whereas the F-N465K protein lost most of the cell-cell fusion activity after exposure to the temperature of 50℃ and about half the activity even at 45℃, the F-N465G and F-N465F proteins exhibited the fusion activity after the heat shock at 55℃. These 2 F proteins maintained nearly whole cell-cell fusion activity after the treatment at 45℃. These results ensure that amino acid 465 with a large molecular volume lowers, whereas ring-type amino acid raises energy barrier for conformational change of the F protein.

Side chain of the ring-type amino acids 465 takes the reverse orientation of that

of non-ring-type amino acids. In the model structure of the pre-fusion F protein, Asn465 in the HR-B domain is located on the surface of the three-helix bundle of the stalk region (Fig. 4A and D). Then mutations of residue 465 were undertaken in the structure model, in which energetically preferred conformations of mutated side chains were explored. Since the F protein is a homotrimer protein, all of the three positions of residue 465 were mutated. As the results, a difference between ring- and non-ring-type residues, excluding Gly, Ala and Pro, was found in their side chain χ_1 conformations, which dominantly determine the side chain orientations against/toward the head region of the pre-fusion form (Fig. 4B). Preferred χ_1 conformations of ring- and non-ring-type side chains were trans and gauche$^+$, respectively. Fig. 4C demonstrates that Lys465 extends the side chain towards Leu354 and Asn462, while imidazoyl group of His465 directs apart from the head region in the close proximity of the helix in the HR-B domain (Fig. 4E). In the model structure, ring-type side chains of residue 465 with the trans conformation of χ_1 angle, extensively cover the surface of the other residues in the helix bundle, particularly that of Lys469 in the same subunit and that of Val467 in the neighboring subunit (Table 1). The side chains of Val467 and ring-type residues at 465 are faced to each other to such an extent that water molecules cannot penetrate between them (Fig. 5).

4. Discussion

The F protein of MV executes refolding from a metastable prefusion form to a highly stable postfusion form to exert its fusion function. Upon activation by the H protein, the three-helix bundle of the HR-B domains dissociates from each other and the HR-A domains folded within the DIII domain in the head region extend to form a long helix bundle, which protrude toward a target cell membrane to initiate the F protein refolding. Zokarkar *et al*. showed that engineered disulfide bond in the membrane-proximal external region located in the stalk of PIV5 F protein inhibits the fusion activity (50). Dissociation and opening of the HR-B bundle should be the first requirement for transition of paramyxovirus F protein from the prefusion to the postfusion conformation. Not a few mutations that alter the fusion activity have been identified around the HR-B and DIII domains. Among them, such mutations in the HR-B domain as T461I, N462K, N462S, N462D, G464W and N465S were all reported to enhance the F protein fusion activity. In this study, an amino acid substitution N465H was identified for the first time as one that eliminates fusion activity.

Here, difference was found in the fusion activity between non-ring- and ring-type residues at position 465 in the HR-B domain of MV F protein. In the case of non-ring-type residues, excluding Gly and Ala, their side chain χ_1 angles preferentially take the gauche$^+$ conformation, which make the bodies of side chains turn toward the head region of the prefusion form, making contacts with Leu354 and Asn462. Prussia *et al.* (10) demonstrated that mutation at 462 could disrupt the hydrophobic interaction between the stalk and head regions, decreasing the energy barrier for dissociation of the HR-B, a necessary step for the large conformational change toward the postfusion form. Leu354 takes part in this hydrophobic interaction along with Thr314, Leu353, Ala367, Ile452, Leu454, Leu457 and Thr461 (Fig. 4A). Asn465 may influence this hydrophobic interaction via contacts with Leu354 and Asn462. Longer side chains can protrude more deeply into the head region and make such contacts more extensive (Fig. 4C and D), which may disturb the hydrophobic interaction between the stalk and head regions and cause destabilization of the molecule lowering the energy barrier for refolding and conferring the F protein the enhanced cell-cell fusion activity. Among the non-ring-type residues at position 465, the F proteins with Gly and Ala demonstrated the lowest cell-cell fusion activity because they can reach neither Leu354 nor Asn462. The fusion activities of Gly and Ala mutants, however, were still higher than those of ring-type residue mutants (see below).

In the case of ring-type residues, excluding Pro, their side chain χ_1 angles preferentially

take the trans conformation, which make the bodies of side chains turn away from the head region of the pre-fusion form, resulting into no contact with Leu354 and Asn462 (Fig. 4E). In the case of Pro, since Pro is often observed to cause a kink in helix, the presence of Pro may change the orientation of helix axes in the three-helix bundle stalk and may change interactions between the stalk and head of the prefusion form. These differential preferences of χ_1 conformations between ring- and non-ring-type side chains have been also indicated by Blaber *et al.* (20) from the statistical analysis of χ_1 angles of residues located in helices of known protein structures.

The results in the present study indicate that mutations of residue 465 to ring-type amino acids increase the thermodynamic stability of the prefusion form. A possible reason for this effect is suggested by analyzing the structure model of the prefusion form (Fig. 5). In the model structure, ring-type side chains of residue 465 with the trans conformation of χ_1 angle, extensively cover the surface of the other residues in the helix bundle, particularly that of Lys469 in the same subunit and Val467 in the neighboring subunit (Table 1), which may contribute to stabilize the helix bundle. The side chains of Val467 and ring-type residues at 465 are faced to each other to such an extent that water molecules cannot penetrate between them (Fig. 5), which may hamper the dissociation of the helices from each other. Lys469 can form a salt-bridge with Glu471 in the neighboring subunit. Existence of bulky ring-type residues at 465 may restrict the movement of the side chain of Lys469, and facilitate the maintenance of the inter-helical salt-bridge with Glu471 (Fig. 5). These effects to stabilize the helix bundle may hinder the conversion from the prefusion to postfusion form. Side chains of Gly and Ala at position 465 are too short to take part in the interaction not only with Leu354 and Asn462 for destabilization of the hydrophobic cluster extending over the stalk and head regions but also with Lys469 and Val467 for stabilization of the helix bundle, suggesting that Gly and Ala at position 465 cause neither enhancement nor suppression of cell-cell fusion activity of the F protein.

Correlations of the fusion activity data were examined with various amino acid indices including those from AAindex database (21) (Table 2). While no significant correlation was seen with secondary structure propensities of amino acids, high correlation coefficients of 0.7 to 0.8 and 0.5 to 0.6 were found with amino acid indices related to side chain flexibility upon ligand binding (22) and those in protein folding (23, 24), respectively. Correlations of the fusion activity with side chain flexibility could indicate that, such amino acid residues that can easily alter their side chain conformations when their environments (surrounding residues, molecules and solvents) change have less possibility to prevent the F protein from passing through the intermediate states on the way of large structural change. In that case, why such a flexible side chain is required at

position 465 remains to be solved.

In Chapter 1, it was demonstrated that intramolecular complementation of the F protein stability between the HR-B and DIII domains results in expression of fusion activity at 37℃, in which stabilization of the F protein by the N465H mutation in the HR-B domain played a key role. Amino acid 465 in the HR-B domain located in the appropriate distance from the head region should modulate fusion activity of the F protein by destabilizing or stabilizing the F protein molecule depending on the orientation and/or the length of its side chain.

5. Tables

TABLE 1. Decrease of the solvent accessible surface area (Å^2) of Val467 and Lys469 on mutating residue 465 from Ala to each of Asn, His, Phe, Try and Trp.

Substituted amino acid (Sub-unit)	(χ_1 angles)	Val467		Lys469	
		Intra-subunit	Inter-subunit	Intra-subunit	Inter-subunit
Asn465					
(A)	*(gauche+)*	0.0	0.0	0.0	0.0
(B)	*(gauche+)*	0.0	0.0	0.0	0.0
(C)	*(gauche+)*	0.0	0.0	0.0	0.0
His465					
(A)	*(trans)*	0.0	6.3	21.8	0.0
(B)	*(trans)*	0.0	0.0	25.8	0.0
(C)	*(trans)*	0.0	9.5	23.7	0.0
Phe465					
(A)	*(trans)*	0.0	9.5	26.5	0.0
(B)	*(trans)*	0.0	1.6	29.0	0.0
(C)	*(trans)*	0.0	11.1	25.3	0.0
Tyr465					
(A)	*(trans)*	0.0	9.5	30.9	0.0
(B)	*(trans)*	0.0	1.6	34.9	0.0
(C)	*(trans)*	0.0	11.1	31.6	0.0
Trp465					
(A)	*(trans)*	0.0	25.3	26.7	0.0
(B)	*(gauche+)*	0.0	0.0	0.0	0.0
(C)	*(trans)*	0.0	30.0	25.3	0.0

TABLE 2. Correlation coefficients of fusion activities with various amino acid indices [a]

	Description of amino acid index	r37	r30	<|r|>	ID
1	Flexibility of sidechain dihedral angles upon ligand binding, from LIG database (1)	0.79	0.83	0.81	_ [b]
2	Sidechain flexibility upon ligand binding, from LIG database (1)	0.70	0.75	0.72	_ [b]
3	Flexibility of sidechain dihedral angles upon ligand binding, from BPK database (1)	0.69	0.71	0.70	_ [b]
4	Optical rotation (2)	0.72	0.62	0.67	FASG760103
5	Principal property value z3 (3)	-0.64	-0.70	0.67	WOLS870103
6	Sidechain flexibility upon ligand binding, from BPK database (1)	0.63	0.65	0.64	_ [b]
7	AA composition of CYT of multi-spanning proteins (4)	0.61	0.57	0.59	NAKH920106
8	Sidechain conformational entropy in protein folding (5)	-0.55	-0.61	0.58	_ [b]
9	Atom-based hydrophobic moment (6)	0.53	0.62	0.58	EISD860102
10	Entire chain compositino of amino acids in nuclear proteins (percent) (7)	0.59	0.56	0.57	FUKS010112
11	Hydrophobicity-related index (8)	0.57	0.54	0.56	KIDA850101
12	Hydrophobic parameter (9)	0.58	0.53	0.55	LEVM760101
13	Sidechain conformational entropy in protein folding (10)	-0.55	-0.55	0.55	_ [b]
14	Entropy of formation (11)	0.46	0.63	0.54	HUTJ700103
15	Average relative fractional occurrence in AL(i) (12)	0.55	0.53	0.54	RACS820103
16	Number of sidechain rotatable bonds (1)	0.51	0.55	0.53	_ [b]
17	Surface composition of amino acids in nuclear proteins (percent) (7)	0.54	0.51	0.53	FUKS010104
18	Entire chain composition of amino acids in intracellular proteins of thermophiles (percent) (7)	0.53	0.51	0.52	FUKS010109
19	Normalized positional residue frequency at helix termini N5 (13)	0.54	0.47	0.51	AURR980110
20	3D-1D scores for the P2 Helix environment class (14)	0.53	0.48	0.51	_ [b]
21	3D-1D scores for the E Sheet environment class (14)	-0.43	-0.57	0.50	_ [b]
22	Free energy in alpha-helical region (15)	-0.53	-0.47	0.50	MUNV940102
23	Normalized frequency of turn (16)	-0.50	-0.50	0.50	CRAJ730103
24	3D-1D scores for the P2 Sheet environment class (14)	0.49	0.51	0.50	_ [b]
25	Normalized positional residue frequency at helix termini C5 (13)	0.52	0.47	0.50	AURR980111

[a] r37 and r30 are correlation coefficients of fusion activities at 37 and 30 °C, respectively, with each amino acid index. <|r|> is the mean of absolute values of r37 and r30, by which the table is sorted. ID is accession code used in AAindex database (17). The indices related to side chain flexibility are highlighted in light-blue. [b] Not registered in AAindex.

6. Figures

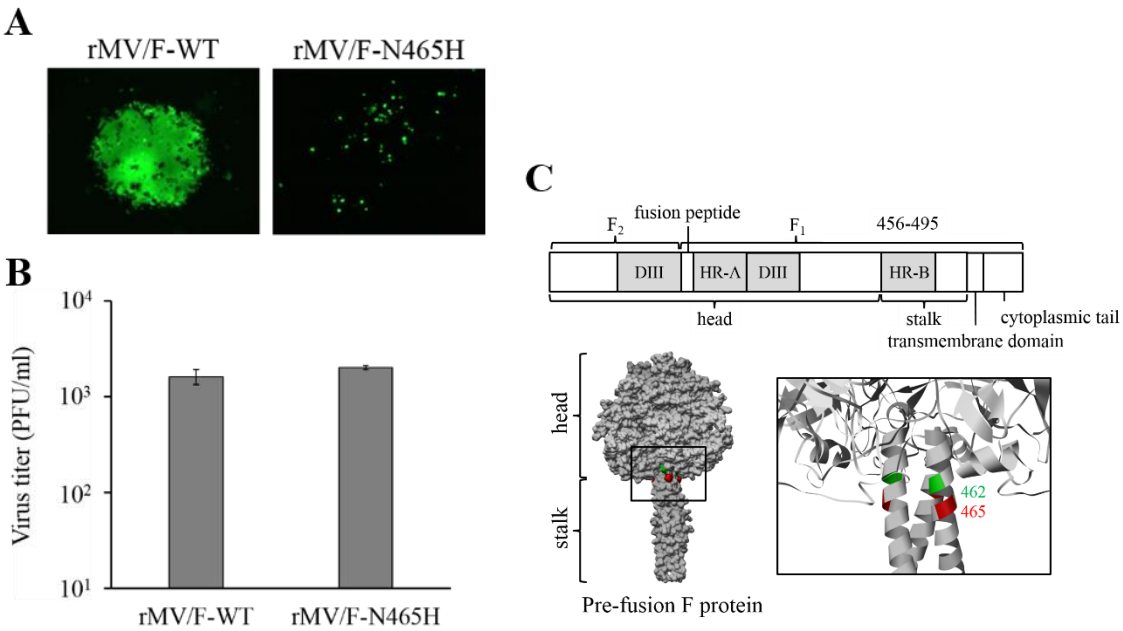

Figure 1.
Abrogation of MV cell-cell fusion by N465H substitution in the F protein. (A) Cytopathic effect of the cells infected with rMV/F-WT or rMV/F-N465H. B95a cells were infected with EGFP-expressing rMV carrying the F-WT protein or F-N465H protein and fixed with 1% paraformaldehyde at 72 h p.i. EGFP expression in the infected cells was observed under a fluorescence microscope. Magnification; x200. (B) Infectious virus titer of the rMV/F-WT and rMV/F-N465H. Vero/hSLAM cells were infected with rMV/F-WT or rMV/F-N465H at an MOI of 0.01. At 72 h p.i., the infectious viruses in the culture medium were titrated. (C) Localization of residue 465 in the pre-fusion form of MV F protein structure. A schematic diagram of the domains of MV F protein (upper panel), surface model of the constructed prefusion form of MV F protein-trimer (lower left panel), and close-up view of N-terminal region of the HR-B domain in ribbon model (lower right panel) are shown. Residues 465 (marked in red) and 462 (marked in green) are located side by side in the HR-B stalk domain.

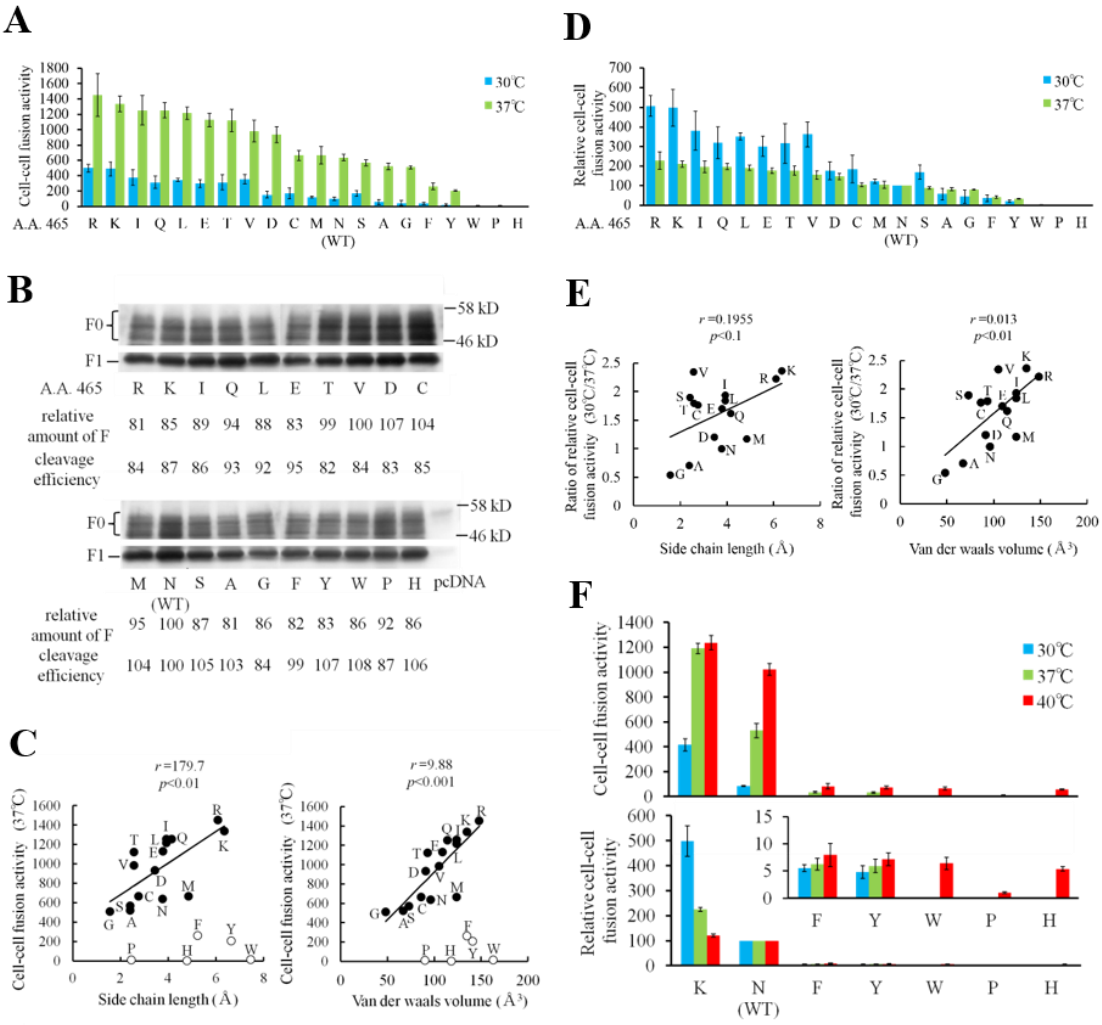

Figure 2.

Correlation of cell-cell fusion activity with the molecular volume of amino acid 465 in the F protein. (A) Cell-cell fusion activities of the 465-mutated F proteins. Vero cells were transfected with the plasmid expressing one of the 465-mutated F proteins together with the H protein-expressing plasmid and incubated at 37℃. At 24 h posttransfection, Vero/SLAM cells were overlaid onto the Vero cells and 100 μ M cycloheximide was added. These cells were further incubated at 37℃ for 12 h, or transferred to 30℃ and incubated for 18 h, followed by fixation with paraformaldehyde and staining with crystal violet. The numbers of syncytia and nuclei in each syncytium were counted under microscope, and cell-cell fusion activity is determined by multiplying these two parameters. Green, cell-cell fusion activities at 37℃; blue, those at 30℃. (B) Cell surface expression and cleavage efficiency of the 465-mutated F proteins. Vero cells were transfected with the 465-mutated F proteins-expressing plasmids, biotinylated at 24 h posttransfection, and lysed. Biotinylated cell surface proteins were precipitated with streptavidin-coated Sepharose beads, and subjected to immunoblot analysis using rabbit antibody against the F protein, followed by determination of the intensity of each F protein band using ImageJ software (http://rsbweb.nih.gov/ij/index.html). Total amounts (combined amount of the F1 subunit and uncleaved F0 protein) of the cell surface-expressed 465-mutated F proteins were shown relative to that of the F-WT protein. Cleavage efficiency was evaluated as the ratio of the F1 subunit to total amount of the F protein. (C) Correlation of cell-cell fusion activity of the F protein with the molecular volume of residue 465. Cell-cell fusion activity of the 465-mutated F protein at 37℃ in (A) was plotted against the length of the side chain (left panel) or Van der Waals volume (right panel) of the residue 465. Correlations were evaluated by Spearman's correlation coefficient for the non-ring-type amino acids (closed circle). Linear regression line is shown as a black line. Five ring-type amino acids were excluded from the evaluation (open circle).

(D) Relative cell-cell fusion activities of the 465-mutated F proteins to that of the F-WT protein. Cell-cell fusion activities of the 465-mutated F proteins at 37℃ and 30℃ in (A) were normalized to the values for the F-WT protein at 37℃ and 30℃, respectively. (E) Correlation of the enhanced relative cell-cell fusion activities of the 465-mutated F proteins at 30℃ with the molecular volume of amino acid 465. Ratio of relative cell-cell fusion activities of the 465-mutated F proteins at 30℃ to those at 37℃ in (D) was plotted against the length of the side chain (left panel) and Van der Waals volume (right panel) of amino acid 465. Correlations were evaluated by Spearman’ s correlation coefficient. Linear regression line is shown as a black line. Ring-type amino acids were excluded from the evaluation. (F) Stimulation of cell-cell fusion activities of the 465-mutated F proteins possessing a ring-type amino acid at higher temperature. Vero cells were transfected with the plasmid expressing a 465-mutated F protein carrying the ring-type amino acid with the H protein-expressing plasmid and incubated at 37℃. At 24 h posttransfection, the Vero cells were overlaid with Vero/SLAM cells, then continuously incubated for 18 h at 30℃ (blue), for 12 h at 37℃ (green) or for 12 h at 40℃ (red), in the presence of 100 μM cycloheximide. Cell-cell fusion activity was quantified as described in (A) (upper panel) and normalized to the value of the F-WT protein at respective temperature as in (D) (lower panel). Relative cell-cell fusion activities of the 465-mutated F proteins with ring-type amino acids were enlarged (inside the lower panel).

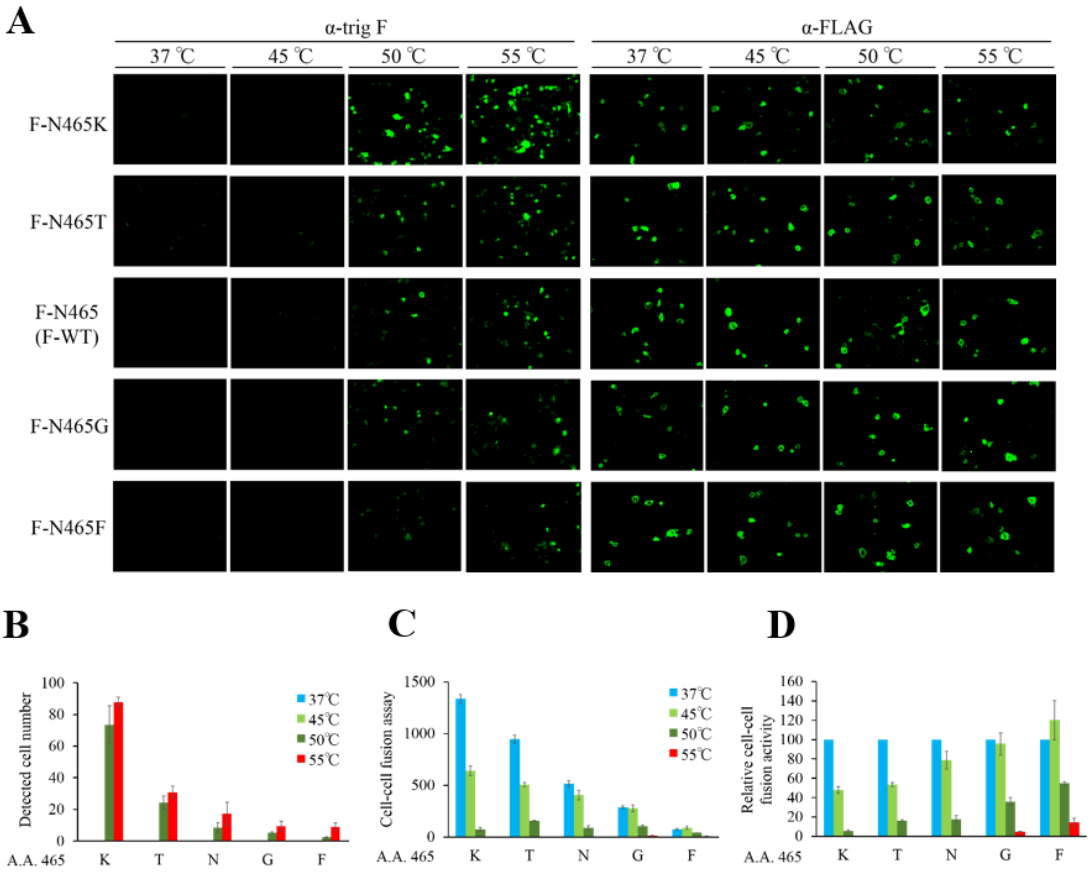

Figure 3.

Evaluation of thermodynamic stability of the 465-mutated F proteins using anti-trig F MAb. (A) Detection of the triggered structure of the F protein. Vero cells were transfected with the plasmid expressing one of the 465-mutated F proteins and incubated at 37℃. At 24 h posttransfection, transfected cells were heat treated at 45℃, 50℃ or 55℃ for 45 min. Subsequently, unfixed and unpermeabilized cells were stained with anti-trig F or anti-FLAG MAb for 1 h at 4℃ followed by incubation with Alexa Fluor 488-conjugated secondary antibody. Images of the positive cells were captured with fluorescence microscope. (B) The number of cells reactive to the anti-trig F MAb. Positive cells in (A) were counted under fluorescence microscope. (C) Cell-cell fusion activities of the 465-mutated F proteins remaining after the heat treatment. Vero cells were transfected with the plasmid expressing one of the 465-mutated F proteins together with the H protein-expressing plasmid and incubated at 37℃. At 24 h posttransfection, the transfected cells were heat treated at the indicated temperature for 45 min and were overlaid with Vero/SLAM cells in the presence of 100 μ M cycloheximide. After further incubation for 12 h at 37℃, cells were fixed with paraformaldehyde and cell-cell fusion activity was quantified as described in Fig. 2A. (D) Relative cell-cell fusion activities of the 465-mutated F proteins. Cell-cell fusion activities in (C) were normalized to the value of each F protein treated at 37℃.

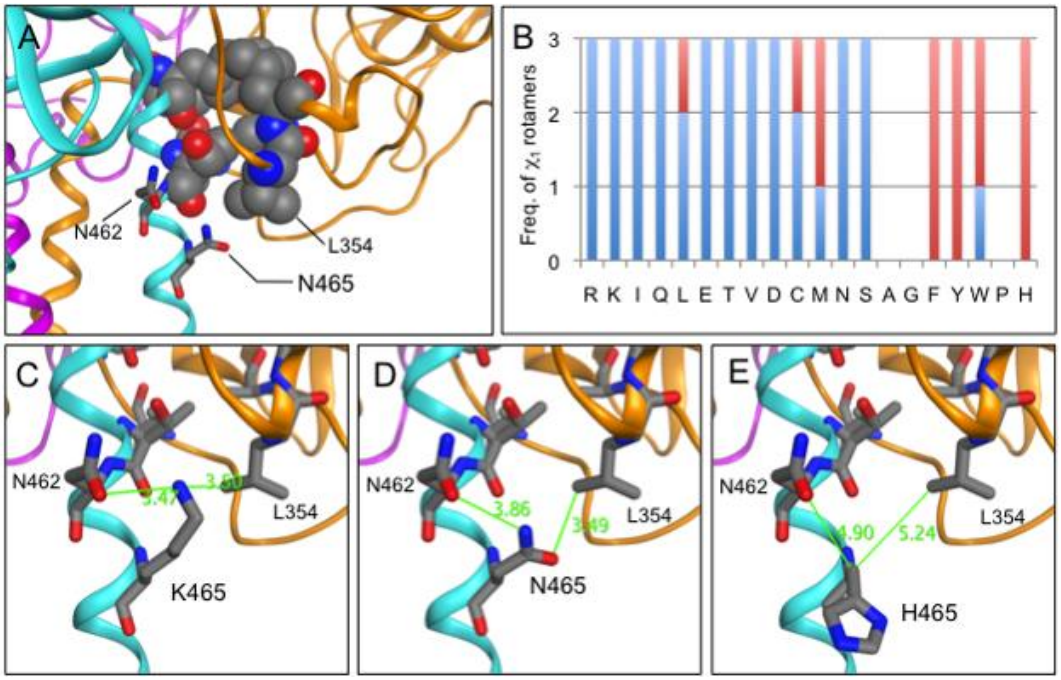

Figure 4.
Orientation of mutated side chains at position 465 in the structure model of MV F protein pre-fusion form. (A) Location of Asn465. Main chains depicted in ribbon model are colored by subunit. Asn462 and Asn465 depicted in stick model, and Thr314, Leu353, Leu354, Ala367, Ile452, Leu454, Leu457 and Thr461 in space-filling model are colored by atom. Residues shown in space-filling model constitute the hydrophobic cluster between the stalk and head regions of the pre-fusion form. (B) Frequencies of side chain χ1 rotamers of mutated amino acid 465. Out of the three mutation sites one for each subunit in the homotrimer F protein, the number of such sites that take the gauche+ (blue) or trans (red) conformation as the most energetically preferred χ1 angle in the model structure is shown for each mutant. (C-E) Conformation of the side chain at position 465. Main chains depicted in ribbon model are colored by subunit, and Leu354, Asn462 and Asn465 are in stick model. The most energetically preferred conformation is shown for each side chain. The preferred χ1 rotamers for Lys465, Asn465 and His465 are gauche+, gauche+ and trans, respectively. The nearest distances between side chains from residue 465 to Leu354 and Asn462 are shown in green.

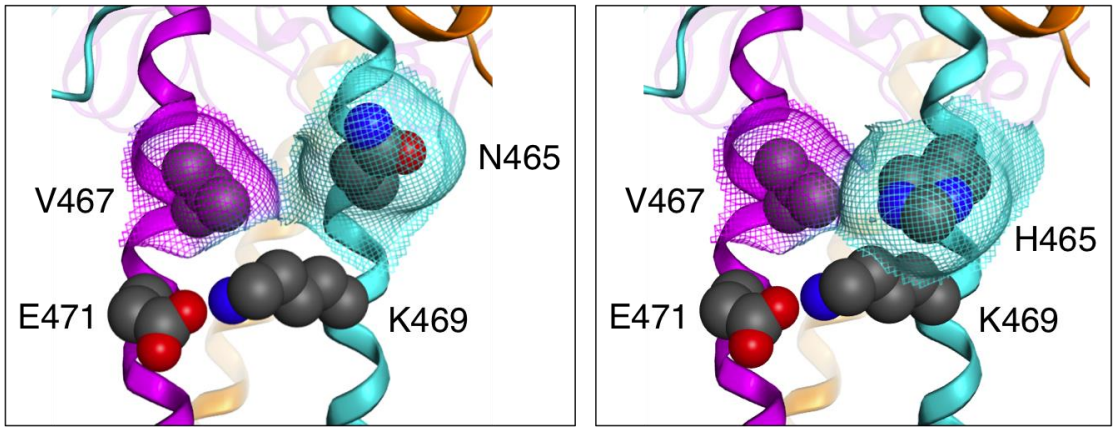

Figure 5.
Contribution of residue 465 to the inter-helix interaction. Main chains are depicted in ribbon model colored by subunit. Side chains of Asn465, His465, Val467, Lys469 and Glu471 are depicted in space-filling model colored by atom. Solvent accessible surface area of Asn465, His465 and Val467 are depicted in wire-netting model colored by subunit, indicating that solvent molecules can penetrate between Val467 and Asn465, but not between Val467 and His465.

ACKNOWLEDGMENT

Many thanks to Dr. Y. Yangi for providing Vero/hSLAM cells and p(+)MV323-EGFP, to Dr. M. Takeda for providing pCITE-IC-N, pCITE-IC-PΔC and pCITEko9301B-L, to Drs. N. Ito and M. Sugiyama for providing the BHK/T7-9 cells, to Dr. M. Ehnlund for 16AG5 antibody and to Dr. B. Moss for providing vTF7-3. This work was supported in part by Grants-in-Aid for Scientific Research from the Japan Society for the Promotion of Science (Grant No. 24591589), the Special Research Program for Prion Disease and Slow Virus Infection from the Ministry of Health, and the Platform for Drug Design, Informatics, and Structural Lifescience (PDIS) from the Ministry of Education, Culture, Sports, Science and Technology, Japan.

REFERENCES

1. **Lamb RA, Parks GD.** 2007. Paramyxoviridae: the viruses and their replication, p 1449–1496. In Knipe DM, Howley PM, Griffin DE, Lamb RA, Martin MA, Roizman B, Straus SE (ed), Fields virology, 5th ed. Lippincott Williams & Wilkins, Philadelphia, PA.
2. **Choppin, PW.** 1984. Membrane proteins and virus virulence. Trans. Am. Clin. Climatol. Assoc. **95**:138 –156.
3. **Griffin DE.** 2007. Measles virus, p. 1551–1585. *In* D. M. Knipe, P. M. Howley, D.E. Griffin, R. A. Lamb, M. A. Martin, B. Roizman, and S. E. Straus (ed.), Fields virology, 5th ed. Lippincott Williams & Wilkins, Philadelphia, PA.
4. **Tatsuo H, Ono N, Tanaka K, Yanagi Y.** 2000. SLAM (CDw150) is a cellular receptor for measles virus. Nature **406**:893– 897.
5. **Yanagi Y, Takeda M, Ohno S.** 2006. Measles virus: cellular receptors, tropism and pathogenesis. J. Gen. Virol. **87**:2767–2779.
6. **Mühlebach MD, Mateo M, Sinn PL, Prüfer S, Uhlig KM, Leonard VHJ, Navaratnarajah CK, Frenzke M, Wong XX, Sawatsky B, Ramachandran S, McCray PB, Cichutek K, von Messling V, Lopez M, Cattaneo R.** 2011. Adherens junction protein nectin-4 is the epithelial receptor for measles virus. Nature **480**:530 –534.
7. **Noyce RS, Bondre DG, Ha MN, Lin L-T, Sisson G, Tsao M-S, Richardson CD.** 2011. Tumor cell marker PVRL4 (Nectin 4) is an epithelial cell receptor for measles virus. PLoS Pathog. **7**:e1002240. doi:10.1371/journal.ppat.1002240.
8. **Wild TF, Malvoisin E, Buckland R.** 1991. Measles virus: both the haemagglutinin and fusion glycoproteins are required for fusion. J. Gen. Virol. **72**:439–442.
9. **Bolt G, Pedersen I-R.** 1998. The role of subtilisin-like proprotein convertases for cleavage of the measles virus fusion glycoprotein in different cell types. Virology. **252**:387–398.
10. **Russell CJ, Kantor KL, Jardetzky TS, Lamb RA.** 2003. A dual-functional paramyxovirus F protein regulatory switch segment: activation and membrane fusion. J. Cell Biol. **163**:363–374.
11. **Plemper RK, Brindley MA, Iorio RM.** 2011. Structural and mechanistic studies of measles virus illuminate paramyxovirus entry. PLoS Pathog. **7**:e1002058.
12. **Ader N, Brindley M, Avila M, Örvell C, Horvat B, Hiltensperger G, Schneider-Schaulies J, Vandevelde M, Zurbriggen A, Plemper RK, Plattet P.** 2013. Mechanism for active membrane fusion triggering by morbillivirus attachment

protein. J. Virol. **87**:314–326.

13. **Hashiguchi T, Ose T, Kubota M, Maita N, Kamishikiryo J, Maenaka K, Yanagi Y.** 2011. Structure of the measles virus hemagglutinin bound to its cellular receptor SLAM. Nat. Struct. Mol. Biol. **18**:135–141.
14. **Apte-Sengupta S, Negi S, Leonard VHJ, Oezguen N, Navaratnarajah CK, Braun W, Cattaneo R.** 2012. Base of the measles virus fusion trimer head receives the signal that triggers membrane fusion. J. Biol. Chem. **287**:33026–33035.
15. **Brindley MA, Takeda M, Plattet P, Plemper RK.** 2012. Triggering the measles virus membrane fusion machinery. Proc. Natl. Acad. Sci. USA. **109**:E3018–3027.
16. **Navaratnarajah CK, Negi S, Braun W, Cattaneo R.** 2012. Membrane fusion triggering: three modules with different structure and function in the upper half of the measles virus attachment protein stalk. J. Biol. Chem. **287**:38543–38551.
17. **Yin H-S, Wen X, Paterson RG, Lamb RA, Jardetzky TS.** 2006. Structure of the parainfluenza virus 5 F protein in its metastable, prefusion conformation. Nature **439**:38–44.
18. **Yin H-S, Paterson RG, Wen X, Lamb RA, Jardetzky TS.** 2005. Structure of the uncleaved ectodomain of the paramyxovirus (hPIV3) fusion protein. Proc. Natl. Acad. Sci. USA **102**:9288–9293.
19. **Prussia AJ, Plemper RK, Snyder JP.** 2008. Measles virus entry inhibitors: A structural proposal for mechanism of action and the development of resistance. biochem. **47:**13573–13583.
20. **Bose S, Heath CM, Shah PA, Alayyoubi M, Jardetzky TS, Lamb RA.** 2013. Mutations in the parainfluenza virus 5 fusion protein reveal domains important for fusion triggering and metastability. J. Virol. **87**:13520–13531.
21. **Avila M, Alves L, Khosravi M, Ader-Ebert N, Origgi F, Schneider-Schaulies J, Zurbriggen A, Plemper RK, Plattet P.** 2014. Molecular determinants defining the triggering range of prefusion F complexes of canine distemper virus. J. Virol. **88**:2951–2966.
22. **Jardetzky TS, Lamb RA.** 2014. Activation of paramyxovirus membrane fusion and virus entry. Current Opinion in Virology. **5**:24–33.
23. **Bose S, Song AS, Jardetzky TS, Lamb RA.** 2014. Fusion activation through attachment protein stalk domains indicates a conserved core mechanism of paramyxovirus entry into cells. J. Virol. **88**:3925–3941.
24. **Wild TF, Fayolle J, Beauverger P, Buckland R.** 1994. Measles virus fusion: role of the cysteine-rich region of the fusion glycoprotein. J. Virol. **68**:7546–7548.
25. **Plemper RK, Lakdawala AS, Gernert KM, Snyder JP, Compans RW.** 2003.

Structural features of paramyxovirus F protein required for fusion initiation. Biochemistry **42**:6645–6655.

26. **Plemper RK, Compans RW.** 2003. Mutations in the putative HR-C region of the measles virus F2 glycoprotein modulate syncytium formation. J. Virol. **77**:4181–4190.
27. **Plemper RK, Erlandson KJ, Lakdawala AS, Sun A, Prussia A, Boonsombat J, Aki-Sener E, Yalcin I, Yildiz I, Temiz-Arpaci O, Tekiner B, Liotta DC, Snyder JP, Compans RW.** 2004. A target site for template-based design of measles virus entry inhibitors. Proc. Natl. Acad. Sci. USA **101**:5628–5633.
28. **Doyle J, Prussia A, White LK, Sun A, Liotta DC, Snyder JP, Compans RW, Plemper RK.** 2006. Two domains that control prefusion stability and transport competence of the measles virus fusion protein. J. Virol. **80**:1524–1536.
29. **Okada H., Itoh M., Nagata K., Takeuchi K.** 2009. Previously unrecognized amino acid substitutions in the hemagglutinin and fusion proteins of measles virus modulate cell-cell fusion, hemadsorption, virus growth, and penetration rate. J. Virol. **83**:8713–8721.
30. **Watanabe S, Shirogane Y, Suzuki SO, Ikegame S, Koga R, Yanagi Y.** 2013. Mutant fusion proteins with enhanced fusion activity promote measles virus spread in human neuronal cells and brains of suckling hamsters. J. Virol. **87**:2648–2659.
31. **Ono N., Tatsuo H., Hidaka Y., Aoki T., Minagawa H., Yanagi Y.** 2001. Measles viruses on throat swabs from measles patients use signaling lymphocytic activation molecule (CDw150) but not CD46 as a cellular receptor. J Virol. **75**:4399–4401.
32. **Ito N, Takayama-Ito M, Yamada K, Hosokawa J, Sugiyama M, Minamoto N.** 2003. Improved recovery of rabies virus from cloned cDNA using a vaccinia virus-free reverse genetics system. Microbiol. Immunol. **47**:613–617.
33. **Seki F, Yamada K, Nakatsu Y, Okamura K, Yanagi Y, Nakayama T, Komase K, Takeda M.** 2011. The SI strain of measles virus derived from a patient with subacute sclerosing panencephalitis possesses typical genome alterations and unique amino acid changes that modulate receptor specificity and reduce membrane fusion activity. J. Virol. **85**:11871–11882.
34. **Wakimoto H, Shimodo M, Satoh Y, Kitagawa Y, Takeuchi K, Gotoh B, Itoh M.** 2013. F-actin modulates measles virus cell-cell fusion and assembly by altering the interaction between the matrix protein and the cytoplasmic tail of hemagglutinin. J. Virol. **87**:1974–1984.
35. **Fuerst TR, Niles EG, Studier FW, Moss B.** 1986. Eukaryotic transient-expression system based on recombinant vaccinia virus that synthesizes bacteriophage T7 RNA polymerase. Proc. Natl. Acad. Sci. USA. **83**:8122–8126.

36. **Takeda M, Takeuchi K, Miyajima N, Kobune F, Ami Y, Nagata N, Suzaki Y, Nagai Y, Tashiro M.** 2000. Recovery of pathogenic measles virus from cloned cDNA. J. Virol. **74**:6643–6647.
37. **Itoh M, Shibuta H, Homma M.** 1987. Single amino acid substitution of Sendai virus at the cleavage site of the fusion protein confers trypsin resistance. J. Gen. Virol. **68**: 2939–2944.
38. **Sheshberadaran H, Norrby E, Mccullough KC, Claes WC, Orvell C.** 1986. The antigenic relationship between measles, canine distemper and rinderpest viruses studied with monoclonal antibodies. J. Gen. Virol. **67**:1381–1392.
39. **Lüthy R, Bowie JU, Eisenberg D.** 1992. Assessment of protein models with three-dimensional profiles. Nature. **356**:83–85.
40. **Russell CJ, Jardetzky TS, Lamb RA.** 2001. Membrane fusion machines of paramyxoviruses: capture of intermediates of fusion. EMBO J. **20**:4024–4034.
41. **Kim YH, Donald JE, Grigoryan G, Leser GP, Fadeev AY, Lamb RA, DeGrado WF.** 2011. Capture and imaging of a prehairpin fusion intermediate of the paramyxovirus PIV5. Proc. Natl. Acad. Sci. USA. **108**:20992–20997.
42. **Ayata M, Takeuchi K, Takeda M, Ohgimoto S, Kato S, Sharma LB, Tanaka M, Kuwamura M, Ishida H, Ogura H.** 2010. The F gene of the osaka-2 strain of measles virus derived from a case of subacute sclerosing panencephalitis is a major determinant of neurovirulence. J. Virol. **84**:11189–11199.
43. **Plattet P, Langedijk JP, Zipperle L, Vandevelde M, Orvell C, Zurbriggen A.** 2009. Conserved leucine residue in the head region of morbillivirus fusion protein regulates the large conformational change during fusion activity. Biochemistry **48**:9112–9121.
44. **Kawashima S, Pokarowski P, Pokarowska M, Kolinski A, Katayama T, Kanehisa M**. 2008. AAindex: amino acid index database, progress report 2008. Nucleic Acids Res. **36**:202–205.
45. **Najmanovich R, Kuttner J, Sobolev V, Edelman M.** 2000. Side-Chain Flexibility in Proteins Upon Ligand Binding. Proteins. **39**:261–268.
46. **Nakashima H, Nishikawa K.** 1992. The amino acid composition is different between the cytoplasmic and extracellular sides in membrane proteins. FEBS Lett. **303**:141–146.
47. **Pickett SD, Sternberg MJE.** 1993. Empirical scale of side-chain conformational entropy in protein folding. J. Mol. Biol. **231**:825–839.
48. **Bowie JU, Lüthy R, Eisenberg D.** 1991. A method to identify protein sequences that fold into a known three-dimensional structure. Science **253**:164–170.

49. **Griffin, DE.** 2013. Measles virus, p 1042–1069. In Knipe DM, Howley PM, Griffin DE, Lamb RA, Martin MA, Racaniello VR, Roizman B (ed.), Fields virology, 6th ed. vol 1. Lippincott Williams & Wilkins, Philadelphia, PA.
50. **Zokarkar A, Connolly SA, Jardetzky TS, Lamb RA.** 2012. Reversible inhibition of fusion activity of a paramyxovirus fusion protein by an engineered disulfide bond in the membrane-proximal external region. **86**:12397–12401.
51. **Blaber M, Zhang X-J, Lindstrom JD, Pepiot SD, Baase WA, Matthews BW.** 1994. Determination of α-Helix Propensity within the Context of a Folded Protein: Sites 44 and 131 in Bacteriophage T4 Lysozyme. J. Mol. Biol. **235**:600–624.
52. **Abagyan R, Totrov M.** 1994. Biased probability monte carlo conformational searches and electrostatic calculations for peptides and proteins. J. Mol. Biol. **235**:983–1002.
53. **Fasman GD.** 1976. "Handbook of Biochemistry and Molecular Biology", 3rd ed., Proteins - Volume 1, CRC Press, Cleveland.
54. **Wold S, Eriksson L, Hellberg S, Jonsson J, Sjostrom M, Skagerberg B, Wikstrom C.** 1987. Principal property values for six non-natural amino acids and their application to a structure-activity relationship for oxytocin peptide analogues. Can. J. Chem. **65**:1814–1820.
55. **Eisenberg D, McLachlan AD.** 1986. Solvation energy in protein folding and binding. Nature **319**:199–203.
56. **Fukuchi S, Nishikawa K.** 2001. Protein surface amino acid compositions distinctively differ between thermophilic and mesophilic bacteria. J. Mol. Biol. **309**:835–843.
57. **Kidera A, Konishi Y, Oka M, Ooi T, Scheraga A.** 1985. Statistical analysis of the physical properties of the 20 naturally occuring amino acids. J. Prot. Chem. **4**:23–55.
58. **Levitt M.** 1976. A simplified representation of protein conformations for rapid simulation of protein folfing. J. Mol. Biol. **104**:59–107.
59. **Hutchens JO.** 1970. Heat capacities, absolute entropies, and entropies of formation of amino acids and related compounds. In "Handbook of Biochemistry", 2nd ed. (Sober HA. ed.), Chemical Rubber Co., Cleveland, Ohio, pp. B60–B61.
60. **Rackovsky S, Scheraga HA.** 1982. Differential geometry and polymer conformation. 4. Conformational and nucleation properties of individual amino acids. Macromolecules **15**:1340–1346.
61. **Aurora R, Rose G.** 1998. Helix capping. Protein Science **7**:21–38.
62. **Munoz V, Serrano L.** 1994. Intrinsic secondary structure propensities of the amino acids, using statistical phi-psi matrices: comparison with experimental scales.

Proteins **20**:301–311.

63. **Crawford JL, Lipscomb WN, Schellman, CG.** 1973. The reverse turn as a polypeptide conformation in globular proteins. Proc. Natl. Acad. Sci. USA **70**:538–542.
64. **Huang F, Nau WM.** 2003. A Conformational flexibility scale for amino acids in peptides. Angewandte Chemie. **115**:2371–2374.